AD NUMBER

ADB258834

NEW LIMITATION CHANGE

TO

Approved for public release, distribution unlimited

FROM

Distribution authorized to U.S. Gov't. agencies only; Proprietary Info.; Oct 99. Other requests shall be referred to US Army Medical Research and Materiel Comd., Fort Detrick, MD 21702-5012.

AUTHORITY

USAMRMC ltr, 1 Jun 2001.

AD_____

Award Number: DAMD17-97-1-7153

TITLE: Role of the Macrophage Growith Factor, Colony Stimulating Factor-1, in the Etiopathogenesis of Breast Cancer

PRINCIPAL INVESTIGATOR: Jeffrey Pollard, Ph.D.

CONTRACTING ORGANIZATION: Albert Einstein College of Medicine
Bronx, New York 10461

REPORT DATE: October 1999

TYPE OF REPORT: Final

PREPARED FOR: U.S. Army Medical Research and Materiel Command
Fort Detrick, Maryland 21702-5012

NOTICE

USING GOVERNMENT DRAWINGS, SPECIFICATIONS, OR OTHER DATA INCLUDED IN THIS DOCUMENT FOR ANY PURPOSE OTHER THAN GOVERNMENT PROCUREMENT DOES NOT IN ANY WAY OBLIGATE THE U.S. GOVERNMENT. THE FACT THAT THE GOVERNMENT FORMULATED OR SUPPLIED THE DRAWINGS, SPECIFICATIONS, OR OTHER DATA DOES NOT LICENSE THE HOLDER OR ANY OTHER PERSON OR CORPORATION; OR CONVEY ANY RIGHTS OR PERMISSION TO MANUFACTURE, USE, OR SELL ANY PATENTED INVENTION THAT MAY RELATE TO THEM.

LIMITED RIGHTS LEGEND

Award Number: DAMD17-97-1-7153
Organization: Albert Einstein College of Medicine

Those portions of the technical data contained in this report marked as limited rights data shall not, without the written permission of the above contractor, be (a) released or disclosed outside the government, (b) used by the Government for manufacture or, in the case of computer software documentation, for preparing the same or similar computer software, or (c) used by a party other than the Government, except that the Government may release or disclose technical data to persons outside the Government, or permit the use of technical data by such persons, if (i) such release, disclosure, or use is necessary for emergency repair or overhaul or (ii) is a release or disclosure of technical data (other than detailed manufacturing or process data) to, or use of such data by, a foreign government that is in the interest of the Government and is required for evaluational or informational purposes, provided in either case that such release, disclosure or use is made subject to a prohibition that the person to whom the data is released or disclosed may not further use, release or disclose such data, and the contractor or subcontractor or subcontractor asserting the restriction is notified of such release, disclosure or use. This legend, together with the indications of the portions of this data which are subject to such limitations, shall be included on any reproduction hereof which includes any part of the portions subject to such limitations.

THIS TECHNICAL REPORT HAS BEEN REVIEWED AND IS APPROVED FOR PUBLICATION.

Patricia A. Woodend 10/6/03

_____ _____

REPORT DOCUMENTATION PAGE

OMB No. 074-0188

1. AGENCY USE ONLY (Leave blank)	2. REPORT DATE	3. REPORT TYPE AND DATES COVERED
	October 1999	Final (30 Sep 97 - 29 Sep 99)

4. TITLE AND SUBTITLE
Role of the Macrophage Growith Factor, Colony Stimulating Factor-1, in the Etiopathogenesis of Breast Cancer

5. FUNDING NUMBERS
DAMD17-97-1-7153

6. AUTHOR(S)
Jeffrey Pollard, Ph.D.

7. PERFORMING ORGANIZATION NAME(S) AND ADDRESS(ES)
Albert Einstein College of Medicine
Bronx, New York 10461

e-mail:
pollard@aecom.yu.edu

8. PERFORMING ORGANIZATION REPORT NUMBER

9. SPONSORING / MONITORING AGENCY NAME(S) AND ADDRESS(ES)
U.S. Army Medical Research and Materiel Command
Fort Detrick, Maryland 21702-5012

10. SPONSORING / MONITORING AGENCY REPORT NUMBER

11. SUPPLEMENTARY NOTES

12a. DISTRIBUTION / AVAILABILITY STATEMENT
Distribution authorized to U.S. Government agencies only (proprietary information, Oct 99). Other requests for this document shall be referred to U.S. Army Medical Research and Materiel Command, 504 Scott Street, Fort Detrick, Maryland 21702-5012.

12b. DISTRIBUTION CODE

13. ABSTRACT ***(Maximum 200 Words)***

A strong association exists between the over-expression in tumor cells of the mononuclear phagocytic growth factor, colony stimulating factor-1 (CSF-1) and its receptor, the *c-fms* proto-oncogene product, and the progression of human breast cancer. There is also a strong association between the number of tumor associated macrophages (TAMs) and poor prognosis. Since CSF-1 is the major growth factor regulating cells of the mononuclear phagocytic lineage, we hypothesized that CSF-1 regulates the recruitment and function of these TAMS to the tumors. We tested this hypothesis by crossing mice that had increased susceptibility to mammary gland cancers with mice carrying a null mutation in the CSF-1 gene ($Csfm^{op}$). In the CSF-1 deficient mice, the incidence of tumorigenesis was similar to wild-type mice. However, there was a dramatic reduction in the progression of these tumors to the metastatic state in CSF-1 deficient mice. In wild-type mice, this transition was correlated with a dramatic macrophage recruitment to sites of invasion of the tumor through the basement membrane. In contrast, in the CSF-1 deficient mice, the tumors were severely depleted in macrophages and they had not progressed to an invasive state. These results strongly support our hypothesis that CSF-1-regulated TAMs play an important role in breast cancer progression.

14. SUBJECT TERMS
Breast Cancer, IDEA Award

15. NUMBER OF PAGES
37

16. PRICE CODE

17. SECURITY CLASSIFICATION OF REPORT	18. SECURITY CLASSIFICATION OF THIS PAGE	19. SECURITY CLASSIFICATION OF ABSTRACT	20. LIMITATION OF ABSTRACT
Unclassified	Unclassified	Unclassified	Limited

NSN 7540-01-280-5500

Standard Form 298 (Rev. 2-89)
Prescribed by ANSI Std. Z39-18
298-102

FOREWORD

Opinions, interpretations, conclusions and recommendations are those of the author and are not necessarily endorsed by the U.S. Army.

_____ Where copyrighted material is quoted, permission has been obtained to use such material.

_____ Where material from documents designated for limited distribution is quoted, permission has been obtained to use the material.

_____ Citations of commercial organizations and trade names in this report do not constitute an official Department of Army endorsement or approval of the products or services of these organizations.

_✓___ In conducting research using animals, the investigator(s) adhered to the "Guide for the Care and Use of Laboratory Animals," prepared by the Committee on Care and use of Laboratory Animals of the Institute of Laboratory Resources, national Research Council (NIH Publication No. 86-23, Revised 1985).

_____ For the protection of human subjects, the investigator(s) adhered to policies of applicable Federal Law 45 CFR 46.

_✓___ In conducting research utilizing recombinant DNA technology, the investigator(s) adhered to current guidelines promulgated by the National Institutes of Health.

_✓___ In the conduct of research utilizing recombinant DNA, the investigator(s) adhered to the NIH Guidelines for Research Involving Recombinant DNA Molecules.

_____ In the conduct of research involving hazardous organisms, the investigator(s) adhered to the CDC-NIH Guide for Biosafety in Microbiological and Biomedical Laboratories.

Oct 29th 1997

PI - Signature Date

TABLE OF CONTENTS:

INTRODUCTION

There is a strong association between the over-expression in tumor cells of the mononuclear phagocytic growth factor, colony stimulating factor-1 (CSF-1) and its receptor, the *c-fms* proto-oncogene product, and the progression of breast cancer and consequently, with poor prognosis. There is also a strong association between the number of tumor associated macrophages (TAMs) and poor prognosis. Since CSF-1 is the major growth factor regulating cells of the mononuclear phagocytic lineage, we hypothesized that CSF-1 regulates the recruitment and function of these TAMs to the tumor. These TAMs then provide trophic molecules that allowed the tumor to break through their constraining basement membrane and therefore, enhanced their metastatic potential. In this IDEA grant, we proposed to test this hypothesis by crossing mice that had increased susceptibility to mammary gland cancers with mice carrying a null mutation in the CSF-1 gene ($Csfm^{op}$). This enabled us to test the effects of the absence of CSF-1 in the tumor and the consequent lack of TAMs. Our results strongly support the hypothesis that TAMs play an important role in breast cancer progression.

BODY

The central hypothesis of this IDEA grant was that tumor-associated macrophages (TAMs) play an important role in the progression of mammary tumors by providing trophic substances essential for tumor growth. To test this hypothesis, we exploited mice homozygous on heterozygous for a null mutation in the gene for the principal mononuclear phagocytic growth factor, colony stimulating factor-1 (CSF-1) (1). Mice homozygous for this mutation ($Csfm^{op}/Csfm^{op}$) are severely depleted in macrophages in most tissues. The strategy was to cross this mutation onto a tumor susceptible strain such that the tumor would be depleted in macrophages. Consequently, by determining tumor incidence, latency and progression, we can test the hypothesis that macrophage play an important role in tumorigenesis.

Almost all our efforts focused upon one tumor susceptible strain, those expressing polyoma Middle T antigen under the control of the mouse mammary tumor virus (MMTV) promoter (MMTV/PYVmT) (2). This strain was originally chosen because of the high penetrance for incidence and, the short latency for induction of these tumors (Task 2). This analysis resulted in considerably more work than we anticipated because of the nature of the effect of the mutation on the progression of tumors. Nevertheless, the data obtained, strongly supports our original hypothesis and provides important insights into the role of macrophages in the progression of mammary gland carcinomas.

The absence of CSF-1 resulted in a delay in both the local progression and the distant metastasis of mammary tumors.

We analyzed 300 MMTV/PYVmT transgenic mice and non-transgenic littermates using whole-mount of right abdominal mammary glands. Mammary tumors developed in all $Csfm^{op}/Csfm^{op}$ and $+/Csfm^{op}$ PYVmT transgenic mice examined as early as 4 weeks in a manner similar to that previously reported for wild-type transgenic mice (2). No mammary tumors were

found in any of the non-transgenic mice indicating that the development of the tumor was due to the expression of the protooncogene, PYVmT, in the mammary glands of the transgenic mice.

As shown in Fig. 1, the tumor progression in the mammary glands of $+/Csfm^{op}$ transgenic mice had defined stages. At an early age, a single tumor focus was developed in the ducts emanating from the nipple in the $+/Csfm^{op}$ mammary glands (Fig. 1a). Tumor foci were then found on the ducts distant to the nipple (Fig. 1c), and eventually enveloped the entire epithelium (Fig. 1e) and became confluent in the mammary gland (Fig. 1g). Despite the formation of focal tumors in the nipple area in all of the $Csfm^{op}/Csfm^{op}$ mammary glands examined at an early age (Fig. 1b), the further development of the tumor to the distal ducts was delayed. As shown in Fig. 1d and 1h, a large percentage of older $Csfm^{op}/Csfm^{op}$ transgenic mice had only single-focal mammary tumors at a time when most of the $+/Csfm^{op}$ mice at the same stage had already developed confluent mammary tumors (Fig. 1g). Furthermore, among older $Csfm^{op}/Csfm^{op}$ mice that developed multiple mammary tumors, many of them were found to have much fewer foci (Fig. 1f) than $+/Csfm^{op}$ littermates (Fig. 1e). Fig. 2A showed a comparison of multiple mammary tumor development between $Csfm^{op}/Csfm^{op}$ and $+/Csfm^{op}$ MMTV/PYVmT transgenic mice, measured as the percentage of mice that developed tumor foci on the distal ducts at various ages. As shown in the figure, a rapid increase of mice carrying multiple mammary tumors was found in young $+/Csfm^{op}$ mice: The percentage of $+/Csfm^{op}$ mice developed multiple foci increased from 0% at 4 weeks to 80% at 8 weeks. At 8 weeks, the curve reached a plateau in which the percentage of mice developed multiple mammary tumors increased much slower. However, by 14 weeks, all of the $+/Csfm^{op}$ mice examined had developed multiple mammary tumors. In contrast to the $+/Csfm^{op}$ littermates, tumor progression in $Csfm^{op}/Csfm^{op}$ mice was markedly delayed. Firstly, the onset of the multiple tumors was delayed by about two weeks. Secondly, the initial phase of increase of the development of multiple mammary tumors in $Csfm^{op}/Csfm^{op}$ mice was more gradual compared to $+/Csfm^{op}$ mice (Fig. 2A). Importantly, the proportion of mice having multiple tumor foci reached 100% for $+/Csfm^{op}$ at 14 weeks, whereas for $Csfm^{op}/Csfm^{op}$, a plateau level of 60 to 70% multiple-tumor incidence was maintained from 12 to 22 weeks. Taken together, these results indicated that the lack of CSF-1 did not inhibit mammary tumorigenesis but the progression of the tumor from focal to the multiple foci stage was markedly delayed in its absence.

Furthermore, we found that among MMTV/PYVmT transgenic mice developing multiple mammary tumors, fewer foci were found in $Csfm^{op}/Csfm^{op}$ mammary glands than in the $+/Csfm^{op}$ glands at similar tumor progression stages, defined with respect to the initiation of the plateau in Fig. 2A. As shown in Fig. 1f, only two small foci were developed on the ducts distal from the nipple in the mammary gland of a 16 weeks old $Csfm^{op}/Csfm^{op}$ mouse. In contrast, many foci have been developed and distributed into the entire mammary epithelium in $+/Csfm^{op}$ mammary gland from a similar stage (at mid-plateau) (Fig. 1e). In order to compare the multiple foci development between $+/Csfm^{op}$ and $Csfm^{op}/Csfm^{op}$ mice, we have examined mice with multiple tumors at two levels: 1) the percentage of mice in which the tumor became confluent; 2) the foci number in mammary glands in which individual foci could still be identified. Mice from the same tumor progression stages defined with respect to the initiation of the plateau in Fig. 2A were compared (8 to 14 weeks for $+/Csfm^{op}$ and 14 to 20 weeks for $Csfm^{op}/Csfm^{op}$). As shown in figure 2B, at the initial point of the plateau, $+/Csfm^{op}$ and $Csfm^{op}/Csfm^{op}$ mice had a similar

percentage (20%) that developed confluent mammary tumors. However, the percentage *+/Csfm^{op}* mice with confluent tumors increased 5 fold over the next 4 weeks and reached 100% at 12 weeks. In contrast, only a one-fold increase of mice with confluent mammary tumors was found in *Csfm^{op}/Csfm^{op}* mice in the first 2 weeks and no further increase was observed during the period of study. Thus, at 20 weeks, *Csfm^{op}/Csfm^{op}* mice that had developed confluent mammary tumors were 60% lower than *+/Csfm^{op}* mice at 14 weeks. Furthermore, we found that mice had not developed a confluent tumor mass in the mammary glands, the average foci number/gland in *Csfm^{op}/Csfm^{op}* mice during the same tumor progression stage was three-fold less than the number found in *+/Csfm^{op}* mice (Table 1). These results indicated that, in addition to the delayed onset of multiple mammary tumor formation in *Csfm^{op}/Csfm^{op}* mice, the increase of foci number in *Csfm^{op}/Csfm^{op}* mice was inhibited.

Interestingly, we found that even though the progression from focal to multiple mammary tumors was delayed in *Csfm^{op}/Csfm^{op}* mice, the sizes of the primary mammary tumor developed at an early age in the nipple area were comparable to the *+/Csfm^{op}* littermates. Fig. 2C showed the measurement of primary tumors from mammary whole mount preparation. As shown in the figure, no significant differences were found in the sizes of the primary tumors between *+/Csfm^{op}* and *Csfm^{op}/Csfm^{op}* mice from 4 to 14 weeks *(Paired t test.* O: 7.3467e-01). No measurements could be obtained from *+/Csfm^{op}* mice older than 14 weeks since by this age, the density of the tumor were too high to identify the primary tumors on the whole-mount samples. However, as shown in the figure, the *Csfm^{op}/Csfm^{op}* curve continuously increased after 14 weeks following the same slope formed at earlier age suggesting that the growth of the primary tumor was not inhibited in *Csfm^{op}/Csfm^{op}* mammary glands.

To determine whether the lack of CSF-1 also affected the distant metastasis of mammary tumors in *Csfm^{op}/Csfm^{op}* PYVmT transgenic mice, the expression of PYVmT RNA by metastatic mammary tumors in lungs was examined using Northern analysis. Fig. 2D shows PYVmT mRNA levels in lungs in both *+/Csfm^{op}* and *Csfm^{op}/Csfm^{op}* transgenic mice relative to the RNA level in the mammary gland of a 14-week old *+/Csfm^{op}* mouse. The results showed that the PYVmT mRNA level in lungs of both *+/Csfm^{op}* and *Csfm^{op}/Csfm^{op}* between 10 to 14-week of age were not higher than the background level. However, a 10-fold increase of the RNA level was observed in lungs of *+/Csfm^{op}* mice at 18 week. This level was maintained until 22 week when an additional 3-fold increase of the mRNA level occurred. No significant increase of PYVmT mRNA level was observed in *Csfm^{op}/Csfm^{op}* lung at all of the corresponding time points and, even at 22 week of age, the PYVmT mRNA level in *Csfm^{op}/Csfm^{op}* lung was not higher than the background level (Fig. 2D).

Delayed tumor progression in *Csfm^{op}/Csfm^{op}* mammary is partially correlated with delayed mammary gland development.

We have shown that mammary gland development in *Csfm^{op}/Csfm^{op}* mice is abnormal (see later). Consequently, it is possible that the effect on tumorigenesis was caused by this developmental delay. Shown in Fig. 3A is the comparison of mammary epithelial development between *+/Csfm^{op}* and *Csfm^{op}/Csfm^{op}* MMTV/PYVmT transgenic mice. This was measured as the ratio of the length of the epithelial tree (from the nipple to the tip of the longest duct) to that

of the fat pad (from the nipple to the tip of the fat pad). Compared to $+/Csfm^{op}$ mice at the same age, the development of the mammary epithelium in $Csfm^{op}/Csfm^{op}$ mice between 4 to 12 weeks was delayed by about three-weeks. Comparing this result to the mammary tumor progression (Fig. 2A) we found that the delayed onset and the prolonged early increase of $Csfm^{op}/Csfm^{op}$ mice developed multiple mammary tumors was correlated to the delayed epithelial development in the mutant mice. Among older transgenic mice, however, the relationship between epithelial development and tumor progression became more complex. As shown in Fig. 3A, between 10 to 12 weeks, the epithelium reached the end of the fat pad in $+/Csfm^{op}$ mammary gland, whereas in $Csfm^{op}/Csfm^{op}$ mammary gland at 12 week, the mean epithelium/fat pad ratio was still 15% lower. However, 79% of the older $Csfm^{op}/Csfm^{op}$ transgenic mice examined between 10 to 18 weeks, had well-developed mammary epithelium similar to the $+/Csfm^{op}$ littermates (Fig. 1d, 1f and 1h). Among these well-developed $Csfm^{op}/Csfm^{op}$ glands, 33% of tumors remained unifocal (Fig. 1d and 1h) and 42% retained low counts of foci (average 9 foci/gland)(Fig. 1f). In contrast, more than 93% of $+/Csfm^{op}$ transgenic mice examined between 10 to 18 weeks had tumors developed over the entire epithelium (>70 foci/gland). Moreover, by 14 weeks, in most of the $+/Csfm^{op}$ mice, tumor lumps were visible externally whereas a large percentage of $Csfm^{op}/Csfm^{op}$ did not develop visible tumor lumps until 20 weeks. These results suggested that in a large population of older $Csfm^{op}/Csfm^{op}$ MMTV/PYVmT transgenic mice, mammary epithelial development was not the limiting factor in the progression of the mammary tumors.

Delayed tumor progression in $Csfm^{op}/Csfm^{op}$ mammary gland is not due to a lower expression of PYVmT nor to changes in tumor cell proliferation.

To eliminate the possibility that the delayed progression of mammary tumors and distant metastasis was due to lower expression level of the transgene, PYVmT, in the $Csfm^{op}/Csfm^{op}$ mice, the expression level of the PYVmT RNA in $+/Csfm^{op}$ and $Csfm^{op}/Csfm^{op}$ mammary glands were compared. Since the development of the mammary epithelium in $Csfm^{op}/Csfm^{op}$ mice was delayed compared to the $+/Csfm^{op}$ littermates, the expression of PYVmT mRNA in each mammary gland was normalized by keratin 18, an intermediate filament expressed in the epithelium and tumor cells (3). Fig. 3B showed such comparison between $+/Csfm^{op}$ and $Csfm^{op}/Csfm^{op}$ mice from 6 to 14 weeks and no significant differences were found.

We also examined the proliferation rate of the mammary tumor cells to eliminate the possibility that the delayed tumor progression and distant metastasis in $Csfm^{op}/Csfm^{op}$ was due to a slow growth of the tumor cells. BrdU incorporation was employed to label the proliferating tumor cells in the mammary glands of the transgenic mice at eight weeks of age. As shown in Fig. 4A, a similar distribution of BrdU incorporated cells were found in $+/Csfm^{op}$ and $Csfm^{op}/Csfm^{op}$ primary tumors and no significant difference was observed when the densities of BrdU positive cells were compared (fig. 4B).

Increased infiltration of leukocytes and macrophages in $+/Csfm^{op}$ relative to $Csfm^{op}/Csfm^{op}$ mammary glands was followed by more advanced histological tumor progression.

To determine whether the primary tumors in $Csfm^{op}/Csfm^{op}$ glands were less metastatic compared to $+/Csfm^{op}$ littermates, histopathological development of the primary tumors in

130 transgenic mice was examined as summarized in Fig. 6. We have classified the histology of the mammary tumors in MMTV/PYVmT transgenic mice into five developmental stages, from the earliest, proliferative lesion (PL), to the most advanced stage, late carcinoma (LC). In an individual mammary gland, the primary focus was always at the most advanced histologic stage. As shown in Fig. 5 and 6, similar histology of the primary tumors were found in *+/Csfm^{op}* and *Csfm^{op}/Csfm^{op}* mice between 4 to 8 weeks. Comparison of the histology at 7 weeks was shown in Fig. 5a for *+/Csfm^{op}* and Fig. 5b for *Csfm^{op}/Csfm^{op}* mice. However, between nine and ten weeks, a more rapid development occurred in the *+/Csfm^{op}* mammary tumors. At this age, 90% of the mice examined had primary tumors that had developed to carcinoma stage, and half of these were at the latest stage, late carcinoma (LC). In contrast, at the same age, 50% of *Csfm^{op}/Csfm^{op}* mice were found to have carcinoma and one third of these was at LC stage (Fig.6). Furthermore, the pathological difference between *+/Csfm^{op}* and *Csfm^{op}/Csfm^{op}* primary tumors at nine to ten weeks was maintained in older mice. Between 17 to 22 weeks, the primary tumors of all of the *+/Csfm^{op}* mice examined developed to the latest stage (LC) whereas only 63% of *+/Csfm^{op}* littermates were at this stage. These results indicated that despite the growth of the primary tumors in *Csfm^{op}/Csfm^{op}* being comparable to that in *+/Csfm^{op}* littermates, the histopathologic progression of the primary tumors was delayed in *Csfm^{op}/Csfm^{op}* mice older than 9 weeks.

To analyze the tumor histology further, we found that the rapid tumor progression in the *+/Csfm^{op}* at nine to ten weeks was correlated to the increased leukocytic infiltration into the mammary gland tumors. The infiltrating cells had the morphology of granulocytes and monocytes and were first observed surrounding the primary tumors in *+/Csfm^{op}* mammary glands at seven weeks (Fig. 7c). The infiltration became intense at eight to nine weeks and continuously increased in older *+/Csfm^{op}* mice (Fig. 7a, 7g). The intensity of the infiltration was closely related to the pathological progression of the primary tumors. Small amounts of infiltrating cells were often found around the primary tumors at the adenoma stage. However, very little infiltration was found surrounding the primary tumors at the adenoma stage in *+/Csfm^{op}* mice younger than seven weeks, even though an intensive infiltration was often observed at the terminal end buds of the mammary gland at this age. Moreover, the leukocytic infiltration became very intense when the primary tumor developed to early carcinomas. Several histological features were observed in the *+/Csfm^{op}* mammary glands that had leukocytic infiltration. Dense leukocytic infiltration sites were found in tumor foci at sites where the tumor acini had lost their "orderly" structure suggesting that the basement membrane of the acina at the infiltration site had lost their integrity (Fig. 7a). Focally infiltrated tumor cells into the connective tissues were observed in some of the samples (Fig.7g). Cells with mast cell morphology were also found surrounding the blood vessels formed around and in the solid tumors (Fig. 7a). Leukocytic infiltration was also found in *Csfm^{op}/Csfm^{op}* mammary glands but the onset of the infiltration was delayed. A few infiltrating cells were found around primary tumors that had developed to carcinoma stage at 20 weeks (Fig. 7i). Similar to the *+/Csfm^{op}* mice, the infiltration was also correlated to the pathological progression of the primary tumors in *Csfm^{op}/Csfm^{op}* mammary glands, however, compared to tumors developed to the same stage in *+/Csfm^{op}* mammary glands, the infiltration in *Csfm^{op}/Csfm^{op}* glands was much more moderate.

To determine the distribution of macrophages during mammary tumor progression, immunohistochemical analysis using a macrophage lineage specific marker, F4/80, was

employed. We found that an increase in infiltration of F4/80 positive cells was observed in *+/Csfm^{op}* mammary glands at 7 to 8 weeks coincident with the leukocytic infiltration (Fig. 7d). The F4/80 positive cells were often found surrounding the developing tumor foci at adenoma or early carcinoma stage and the infiltration became intense in the late carcinoma stage. Increased infiltration of F4/80 positive cells in the lymph nodes and the connective tissues surrounding the mammary glands were also observed in many *+/Csfm^{op}* mammary glands at seven to ten weeks of age. Morphologically, most of the F4/80 positive cells in *+/Csfm^{op}* mammary glands were dendritic and spread. In contrast to the *+/Csfm^{op}* littermates, very few F4/80 positive cells were detected around the tumor in *Csfm^{op}/Csfm^{op}* mammary glands (Fig. 7f). Unlike the granulocytic infiltration, which became relatively intense in *Csfm^{op}/Csfm^{op}* mammary glands when the primary tumors developed to carcinomas, there was little increase in F4/80 positive cells in these glands. A mild increase of F4/80+ cell infiltration was found in well-differentiated tumors in the *Csfm^{op}/Csfm^{op}* at 20 weeks (Fig. 7j), however, compared to the *+/Csfm^{op}* littermates, the infiltration was still very moderate (Fig. 7h). Morphologically, F4/80 positive cells in *Csfm^{op}/Csfm^{op}* mammary glands were similar to these found in *+/Csfm^{op}* glands.

We found that the distant metastasis in *+/Csfm^{op}* mice was correlated to the histopathological stage of tumor. As shown above, an increase in metastasis, measured by the expression of PYVmT transgene in metastatic mammary tumors in lung, was found in *+/Csfm^{op}* mice at 18 weeks. All of the *+/Csfm^{op}* mice examined for the lung metastasis at this age have developed late carcinoma in mammary glands. In contrast, distant metastasis was not detected in *Csfm^{op}/Csfm^{op}* mice even though the primary mammary tumors had developed to the late carcinoma. Among *Csfm^{op}/Csfm^{op}* mice examined for lung metastasis, 3 out of 5 *Csfm^{op}/Csfm^{op}* mice at 18 weeks were at LC stage and the rest two were at EC stage. All of the *Csfm^{op}/Csfm^{op}* mice (7 mice) examined at 20 to 22 weeks were at LC stage. However, PYVmT RNA expression was not detected in lungs of these mice. Thus metastatic potential strongly correlates with the recruitment of macrophages to the tumor.

These data strongly implicate macrophages in the progression of tumors to late metastatic carcinomas and fulfils the aims of Task 1 and 2. They also provide strong evidence in support of our hypothesis that macrophages play an important role in tumor progression.

It should be noted that we had also proposed that we would test this hypothesis using three other tumor models. This became impractical for a variety of reasons, not least the very large numbers of mice that we needed to analyze to distinguish the effects of macrophage deficiency on tumor progression in the MMTV/ PYVmT mice and the age of the mice that this took to manifest itself. Thus we abandoned the alternative MMTV-cyclin D1 tumor model because of its long latency which would have precluded analysis in the time frame of this grant. As mentioned in our progress report, we had proposed to transplant FMA3A C3H mammary tumors into *Csfm^{op}/Csfm^{op}* mice that had been inbred onto a C3H background. However, these cells were rejected by wild type C3H mice, precluding the use of this approach to analyze the effect of the *Csfm^{op}* mutation on tumorigenicity. This suggests that our mice were either not inbred enough, or that there were minor histocompatibility differences between the C3H mouse strains that we had obtained and the strain from which the cell line had been derived. We attempted to further inbreed our mice beyond N6 but at this point we were unable to propagate

the *Csfm*^{op} mutation. A similar failure was found at the Jackson labs when they tried to inbreed onto a C57/Bl6 background (L. Schultz, personal communication). This was important since we wanted to analyze the tumor development in MTV infected *Csfm*^{op}/*Csfm*^{op} C3H mice (task 1). Preliminary results were encouraging but with the loss of the inbred strain we decided not to pursue this task further. However, the data obtained showing a lower tumor incidence in *Csfm*^{op}/*Csfm*^{op} mice compared to +/*Csfm*^{op} mice was significant and confirmed the extensive analysis of MMTV/PYVmT transgenic mice described above. Thus, task one gave important support to our hypothesis that macrophages play an important role in mammary tumor progression

Expression of CSF-1 in *Csfm*^{op}/*Csfm*^{op} mammary glands accelerated tumor progression.

In Task four we had proposed to test the hypothesis that re-introduction of CSF-1 directly into the mammary glad of *Csfm*^{op}/*Csfm*^{op} would reverse the inhibition of tumorigenesis. If this occurred then we would be able to dissociate the systemic from local effects of the deprivation of CSF-1 on mice. We also planed to have this restoration regulatable by constructing a tetracycline-repressible system so that we could turn off the expression of CSF-1 at defined stages in tumorigenesis by treatment of mice with tetracycline. Therefore, to determine whether the effects of CSF-1 on the progression of the tumor is directly in the mammary gland, lines of transgenic mice expressing CSF-1 under control of the tet operon and with the tet transactivator under the control of MMTV LTR were prepared and bred with MMTV/PYVmT transgenic mice heterozygous for the *Csfm*^{op} mutation.

Mammary tumor progression in 6 *Csfm*^{op}/*Csfm*^{op} mice carrying all of the transgenes (PYVmT/ Ta/CSF-1) and 9 negative control *Csfm*^{op}/*Csfm*^{op} mice carrying MMTV/PYVmT and one of the transgenes (PYVmT/Ta or PYVmT/CSF-1) were examined using mammary gland whole mount analysis. As shown in Fig. 8, whole mount analysis has shown that the percentage of *Csfm*^{op}/*Csfm*^{op}/PYVmT/CSF-1+ mice developed multiple mammary tumors was almost double the control mice (*Csfm*^{op}/*Csfm*^{op} /PYVmT/CSF-1-) suggesting that CSF-1 acts as a local factor promoting the progression of the mammary tumors from focal to multiple stages.

Taken together, the results showed that CSF-1 may act as a local growth factor that may regulate the mammary tumor progression directly or regulate this process through promoting the development of the mammary epithelium.

Absence of CSF-1 results in abnormal postnatal mammary gland development

It became apparent to us during the course of the studies on the role of macrophages in mammary tumorigenesis that the development of the mammary gland was retarded in *Csfm*^{op}/*Csfm*^{op} mice. Indeed, our original hypothesis was predicated upon our publication showing that CSF-1 was required for branching morphogenesis in the mammary gland during pregnancy (4). This led to the suggestion that macrophages provided similar functions during mammary gland growth and tumorigenesis. To understand this role for CSF-1 and macrophages and to extrapolate this to the tumor situation, it became important to define the developmental

defects in the *Csfm^{op}/Csfm^{op}* mice. Consequently, we analyzed mammary glands of the CSF-1 null mutant mice, *Csfm^{op}/Csfm^{op}* mice compared to heterozygote control mice using whole mount preparations of the fourth abdominal mammary glands of mice from 2.5 to 12 weeks of age (Fig. 9). Terminal end bud (TEB) formation, the initial structure for duct elongation, is delayed in *Csfm^{op}/Csfm^{op}* mice (Fig. 10A). At 2.5 weeks of age, the mammary glands of control and mutant mice display the same rudimental branching tree (not shown). In control mice, the first TEBs appear at 3 weeks (Fig. 9, 10A). TEB number in control mice increases up to 7 weeks of age, with a peak at 5 weeks of age when the fat pad is the widest in the lymph node area (Fig. 10A). However, in mutant mice, the onset of TEB formation is delayed by one week, and although increasing to a peak at 5 weeks, is reduced over 2.5 fold compared to wild type mice. In addition, the computation of area under the curve of TEB number indicates that TEB number in *Csfm^{op}/Csfm^{op}* mice throughout postnatal development represent 50 % of TEB number found in control mice. This result shows that not only is mammary gland development delayed in *Csfm^{op}/Csfm^{op}* mice, but it also never catches up with that seen in control mice. The defected TEB number in mutant mice is also illustrated in Fig. 11 showing that certain major ducts display tapered ends instead of the TEBs that end all ducts at the epithelial migration front in control mice (Fig. 13a). Consequently, the mammary gland of *Csfm^{op}/Csfm^{op}* mice has fewer ducts then wild type mice (Fig. 9, 11) .

The more extensive ductal tree in the mammary gland of *+/Csfm^{op}* mice compared to mutant mice is shown by a consistently greater branching number and ductal length (Fig. 10b, 10c) as well as a larger fat pad size throughout the postnatal development (Fig. 9). Between 8 and 9 weeks, the ductal tree of *+/Csfm^{op}* mice filled the whole fat pad, TEBs have disappeared (Fig. 10a, 10g), ducts are much thinner and some secondary ducts resulting from the hormonal estrus cycle influence are formed (Fig. 10, 11e). In contrast, the ductal tree is still growing in *Csfm^{op}/Csfm^{op}* mice at 9 weeks with thick ducts and some TEBs still present (Fig. 9, 10a, 11f, black head arrow). In addition the orientation of ducts in mutant mice is disorganized; ducts are not always migrating towards the tip of the fat pad, instead they are curved and migrating towards a lateral or opposite direction (Fig. 11d, 11f). However, at 12 weeks of age, the ductal tree does fill almost fully the atrophic fat pad. At that age, ducts finally display a mature morphology with a thin diameter (Fig. 11h), nevertheless, the secondary branches remain rare compared to the well-branched out epithelial tree in control mice (Fig. 11g). To ensure that the atrophic epithelial tree in mutant mice was not only due to the result of a small fat pad, we measured the ductal growth relative to the growth of fat throughout postnatal development (Fig 10d). In both control and mutant mice, this ratio tends to converge to 1, indicating that the ductal tree reaches the tip of the fat pad. However, the ductal growth relative to the fat growth from 3 weeks to 11 week of age is significantly greater in control mice versus mutant mice. This difference is particularly important at 3-4 weeks, when the ductal outgrowth is delayed in mutant mice displaying only few TEBs and no increase of ductal length and branching number. These data confirm that the defective ductal growth is not only the result of a smaller fat pad but rather of a defect in epithelial tree development. Taken together, these data show a delay in mammary gland development in CSF-1 null mutant mice that leads to the formation of an abnormal atrophic adult mammary gland, characterized by fewer ducts and minimal branches.

Macrophage recruitment correlates with TEB formation

Since CSF-1 is the major growth factor required in mononuclear phagocyte proliferation, differentiation and recruitment, we addressed the question of whether the defective ductal tree in *Csfm^{op}/Csfm^{op}* mice was due to a macrophage population deficiency in mammary gland. We analyzed macrophage distribution during prepubertal mammary gland development in the CSF-1 null mutant mice and their littermate controls, by performing immunohistochemistry with the antibody anti-F4/80 (5). F4/80 protein was originally identified as a murine macrophage-restricted cells surface marker (5). However, we have found that the anti-F4/80 antibody also cross-reacts with eosinophils in the mammary gland (Fig. 12a, 12b). Among F4/80 positive cells, eosinophils are easily distinguished from macrophages at high power magnification (1000X) by their nuclear shape (polynuclear and often forming a ring for eosinophil and mononuclear for macrophage), their cytoplasmic shape (round for eosinophil and largely spread for macrophage) and their characteristic-Giemsa-positive cytoplasmic granules (Fig. 12a). Double staining of the same TEB section showed the giemsa-positive granule eosinophils (Fig. 12a) as F4/80 positive cells (Fig. 12b). This cross-reactivity has not been previously observed in tissues, most likely due to the paucity of tissue eosinophils in mice under healthy conditions. Nevertheless, previous studies have indicated that bone marrow and peritoneal eosinophils from several strains of mice stained positively with the antibody anti-F4/80 using flow cytometry analysis (6).

Very early in the postnatal development of the mammary gland, at 2.5 weeks of age, from the F4/80 positive cells, macrophages are the only cells abundantly spread out around the nipple area in *+/Csfm^{op}* mice, in contrast to the *Csfm^{op}/Csfm^{op}* mice where F4/80 positive cells are almost completely absent (Fig. 12c, 12d). At 3 weeks of age, when TEBs appear in *+/Csfm^{op}* mice, F4/80 positive cells are recruited around all TEBs at the density of 12.94 +/- 0.46 cells/surface unit (Fig. 12e). Of these F4/80 positive cells, eosinophils are distributed around the head of TEBs and also colocalize with the macrophages that are found largely at the neck of TEBs. In contrast, in *Csfm^{op}/Csfm^{op}* mice, very few F4/80 positive cells were found around the rudimentary tips of ducts that at this time have not yet formed into TEBs (Fig. 12f). F4/80 positive cells present in the mammary gland are most likely of two origins beside their vascular origin, the connective tissue adjacent to the fat pad and the lymph node, consistent with intense F4/80 immunostaining in both these locations in mammary glands of *+/Csfm^{op}* mice (data not shown). In accord with previous studies demonstrating that macrophage populations in lymph node are independent of CSF-1 (7) macrophages are also present in the lymph nodes of CSF-1 null mutant mice but they are absent in the connective tissue (data not shown). Despite their presence in lymph node, macrophages do not appear to migrate from the lymph node into the mammary fat in CSF-1 null mutant mice at 3 weeks of age, and eosinophils are the only F4/80 positive cells found and they are scattered abundantly throughout the fat pad. In control mice, the F4/80 positive cells appear to be released from the lymph node into the fat pads as indicated by their localization at the edge of the capsule of the lymph node in the medullar cord. These cells in the fat pad are distributed equally between macrophages and eosinophils. These data indicate that macrophage and eosinophil recruitment is closely related to TEB formation.

At 5 weeks of age, the density of total F4/80 positive cells associated with TEBs in control mice increased significantly (19.67 +/- 2.43 versus 12.94 +/- 0.46 cells/surface unit at 3

weeks of age) (Fig. 12g, 13). Interestingly, at this later age, F4/80 positive cells are also recruited around the TEBs developed in *Csfm^{op}/Csfm^{op}* mice (Fig. 12h, 13). In both genotypes, approximately 50% of F4/80 positive cells are macrophages, while the other 50% are eosinophils (Fig. 13). However, the total F4/80 positive cell density surrounding TEBs remains significantly lower in mutant mice compared to control mice (10.331 +/- 0.979 in *Csfm^{op}/Csfm^{op}* mice versus 19.67 +/- 2.43 cells/surface unit in +/ *Csfm^{op}* mice). Of these F4/80 positive cells, both macrophage and eosinophil numbers were significantly reduced in mutant mice compared to control mice (Fig. 13).

CSF-1 treatment from birth partially rescues the mammary gland defect in Csfm^{op}/Csfm^{op} mice

In order to determine whether circulating CSF-1 is necessary for ductal outgrowth, we treated the mutant mice and their littermate control mice from birth with a daily injection of 10^6 IU of human recombinant CSF-1. This dose was previously designed to at least maintain circulating concentrations of CSF-1 (7). Following treatment, we examined mammary gland development in *Csfm^{op}/Csfm^{op}* mice. Mice were sacrificed at 5 weeks of age, and immunohistochemistry with the anti F4/80 antibody was performed on the sections of the left abdominal mammary gland whole mounts. After 5 weeks of daily CSF-1 treatment of *Csfm^{op}/Csfm^{op}* mice, even though the total number of F4/80 cells surrounding TEBs did not reach the number in untreated control mice (11.92 +/- 1.33 versus 19.67 +/- 2.43 cells/surface unit), the macrophage number in treated *Csfm^{op}/Csfm^{op}* mice was similar to the number in untreated control mice (9.15 +/- 0.95 versus 9.25 +/- 1.5 cells/surface unit) (Fig. 13). Most of the F4/80 positive cells in CSF-1 treated-mutant mice as well as control mice were identified as macrophages (Fig. 13); and the numbers of eosinophils were strongly decreased and significantly different to the macrophage numbers in both genotypes ($P<0.03$, Fig. 13). In CSF-1 treated *+/Csfm^{op}* mice, even though the number of total F4/80 positive cells decreased compared to the untreated *+/Csfm^{op}* mice (13.81 +/- 1.799 versus 19.67 +/- 2.43 cells/surface unit), the macrophage numbers around TEBs were similar in both situations.

In parallel, the right abdominal mammary gland whole mounts were analyzed as described above. CSF-1 treatment rescued the TEB number and the branching number in *Csfm^{op}/Csfm^{op}* mice, consistent with the rescue of macrophage density around TEBs (Fig. 14a, 14b). However, the ductal length remained low compared to the untreated control mice (Fig. 14c). Similarly, the fat pad size was still reduced in *Csfm^{op}/Csfm^{op}* mice after CSF-1 treatment (not shown), suggesting a close correlation between the control of fatty stroma size and ductal length.

Collectively, our data show the necessity of circulating CSF-1 for macrophage recruitment around TEB leading to a proper TEB and branch formation. This CSF-1 acts indirectly through CSF-1R expressing macrophages, by recruiting them around the growing ducts in the mammary gland. These macrophages appear to play trophic roles either /or by providing growth factors or enzymes that promote matrix remodeling during the outgrowth of the epithelial structures.

KEY RESEARCH ACCOMPLISHMENTS

- This grant was aimed at testing the hypothesis that macrophages play important roles in the progression of mammary gland tumors. Our data provides strong evidence that this is the case and points to a critical role for macrophages in the progression of mammary gland tumors to a metastatic state. This, we believe, is an extremely important result with high relevance for understanding the biology of human tumors.

- Leukocytes are essential for the normal development of the mammary gland. They influence the overall complexity of the mammary gland and determine the role of branching outgrowth.

REPORTABLE OUTCOMES

Research supported by this grant has resulted in three major manuscripts, one submitted and two in the final stages of preparation.

These data were presented in three oral presentations in the Mammary Gland Gordon Conference in the summer of 1999.

Several animal models were developed in this grant period including double transgenics that have CSF-1 under a regulatable promoter; a β-lactoglobulin TGFβ3 transgenic mouse and the *Csfm*^{op} allele carried on various tumor susceptible strains.

CONCLUSIONS

The data obtained in this grant has provided strong support for the hypothesis that tumor associated macrophages (TAMs) are important players in the progression of mammary gland tumors to the metastatic state. Clinical data had suggested that there was a correlation between TAMs and poor prognosis, and we have now provided experimental evidence indicating that there is a causal relationship. We have also developed a model system that can identify the macrophage-derived factors responsible for the progression of these tumors. Inhibition of these actions could profoundly influence the life history of mammary gland cancers and significantly improve prognosis.

REFERENCES

1. Pollard, J.W. and E. R. Stanley. Pleiotropic roles for CSF-1 in development defined by the mouse mutation osteopetrotic. (1996) Adv. Develop. Biochem. 4:153-193.

2. Guy, C.T., Cardiff, R.D. and W. J. Muller. (1992) Induction of mammary tumors by expression of polyomavirus middle T oncogene: a transgenic mouse model for metastatic disease. Mol. Cell. Biol. 12(3):954-61.

3. Oshima, R.G., Baribault, H. and C. Caulin. (1996) Oncogenic regulation and function of keratins 8 and 18. Cancer and Metastasis Reviews 15:445-471.

4. Pollard, J.W. and L. Hennighausan. (1994) Colony stimulating factor-1 is required for mammary gland development during pregnancy. Proc. Natl. Acad. Sci. U.S.A. 91:9312-9316.

5. Austyn, J.M. and S. Gordon. (1981) F4/80, a monoclonal antibody directed specifically against the mouse macrophage. Euro. J. Immunol. 11:805-815.

6. McGarry, M.P. and C.C. Stewart. (1991) Murine eosinophil granulocytes bind the murine macrophage-monocyte specific monoclonal antibody F4/80. J. Leukocyte Biol. 50:471-478.

7. Cecchini, M.G., Dominguez, M.G., Mocci, S., Wetterwald, A., Felix, R., Fleisch, H., Chisholm, O., Hofstetter, W., Pollard, J.W. and E. R. Stanley. (1994) Role of colony stimulating factor-1 in the establishment and regulation of tissue macrophages during post-natal development of the mouse. Development 120:1357-1372.

Figure 1

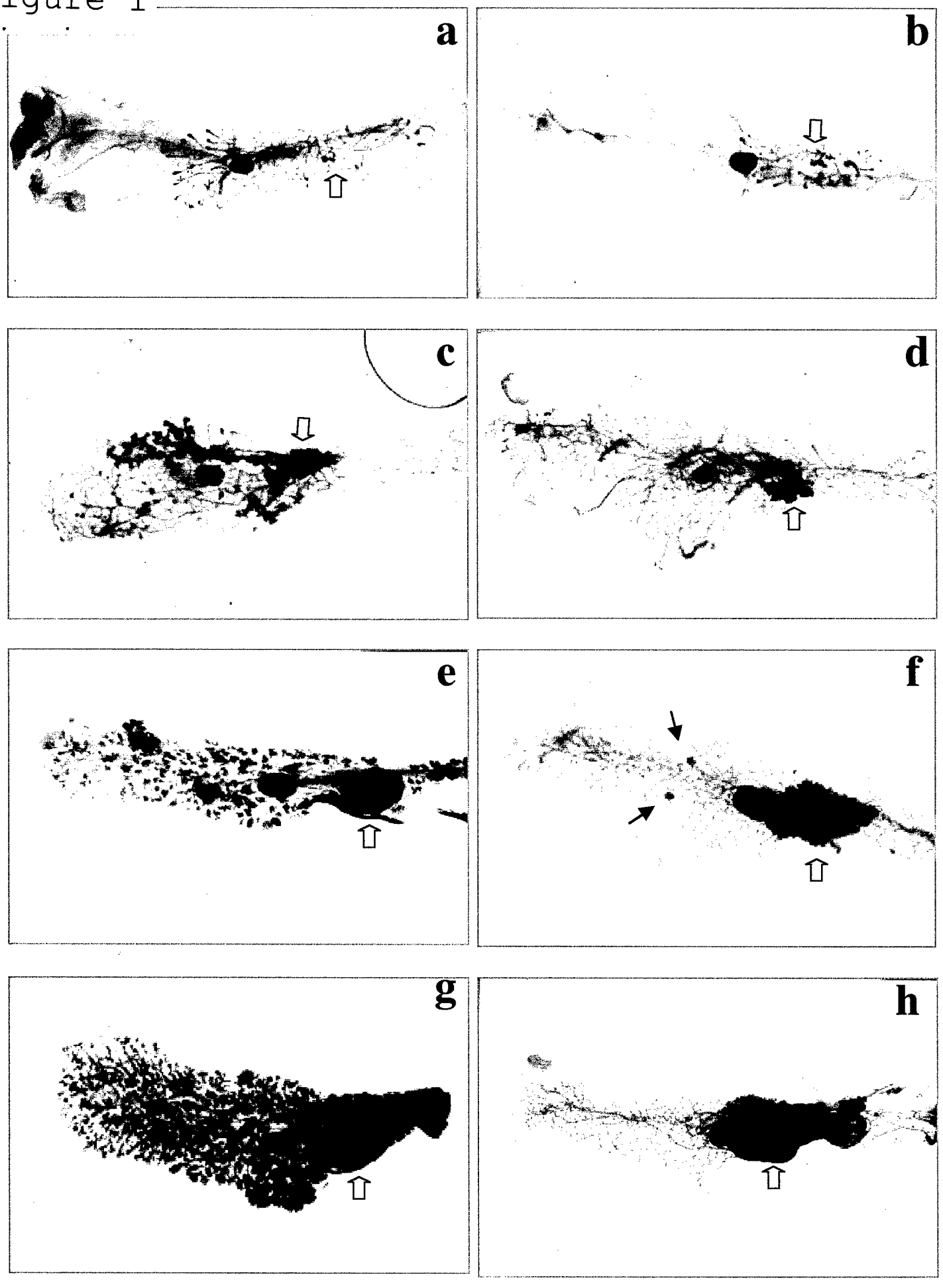

Figure 2

A

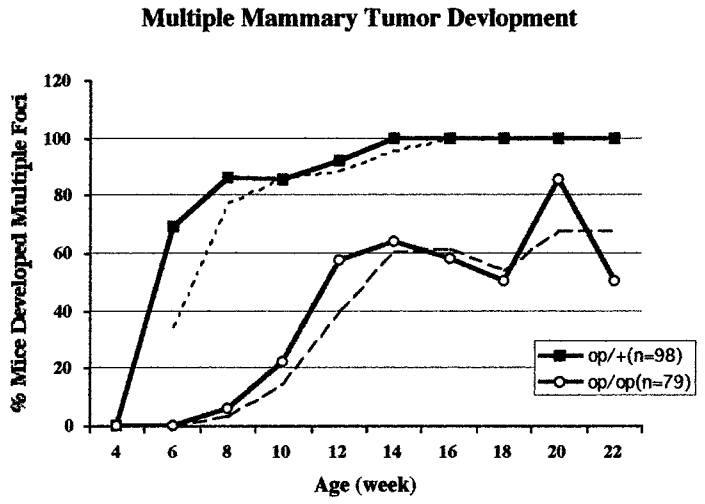

B

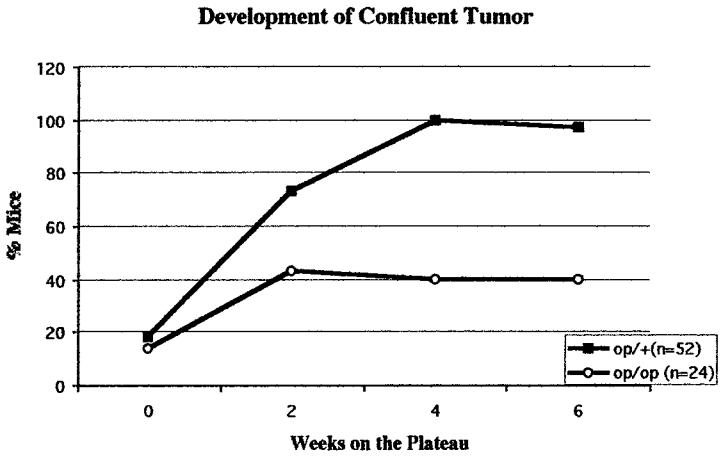

18

C

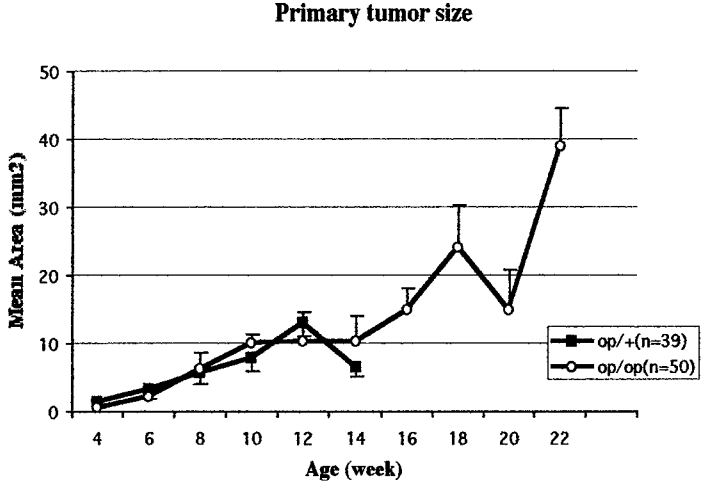

D

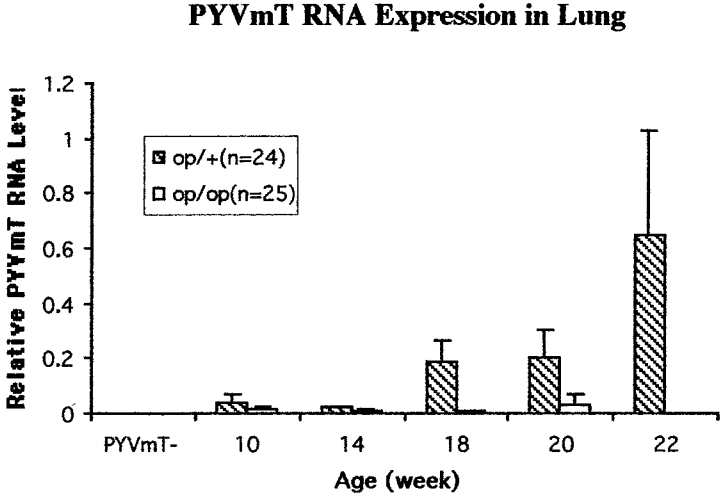

Figure 3

A

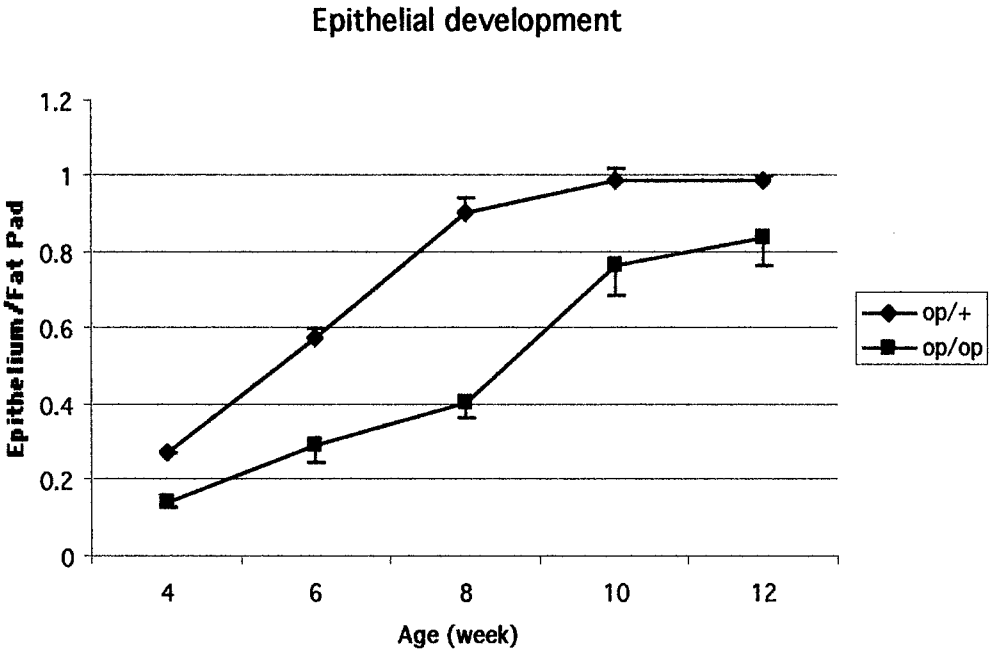
Epithelial development
Epithelium/Fat Pad
1.2
1
0.8
0.6
0.4
0.2
0
4
6
8
10
12
Age (week)
op/+
op/op

B

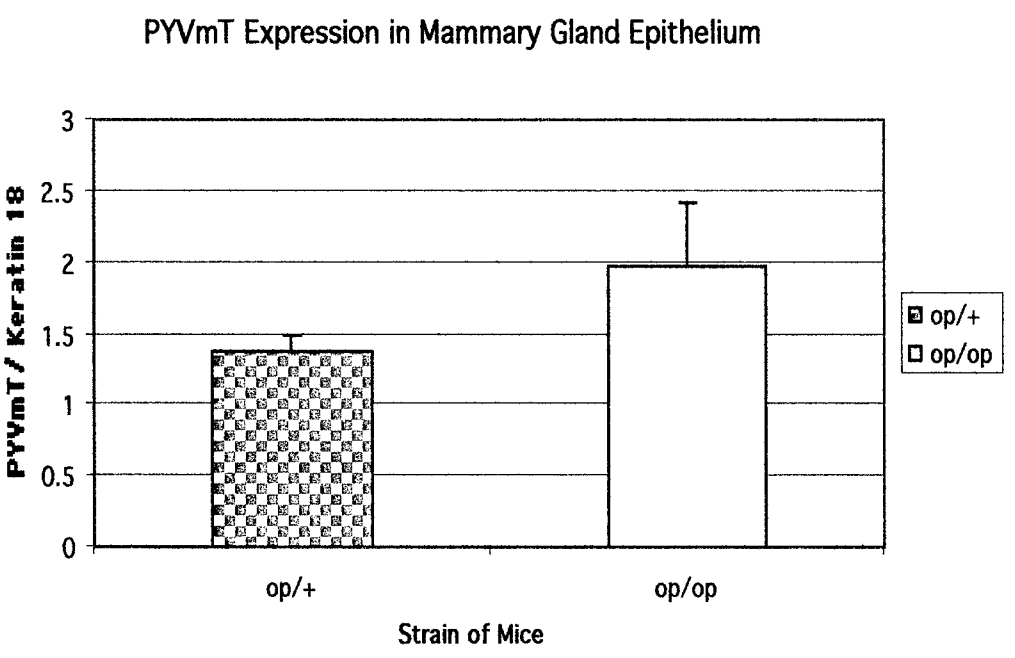
PYVmT Expression in Mammary Gland Epithelium
PYVmT / Keratin 18
3
2.5
2
1.5
1
0.5
0
op/+
op/op
Strain of Mice
op/+
op/op

Figure 4

BrdU Incorporation in Mammary Tumors at 8 weeks

A.

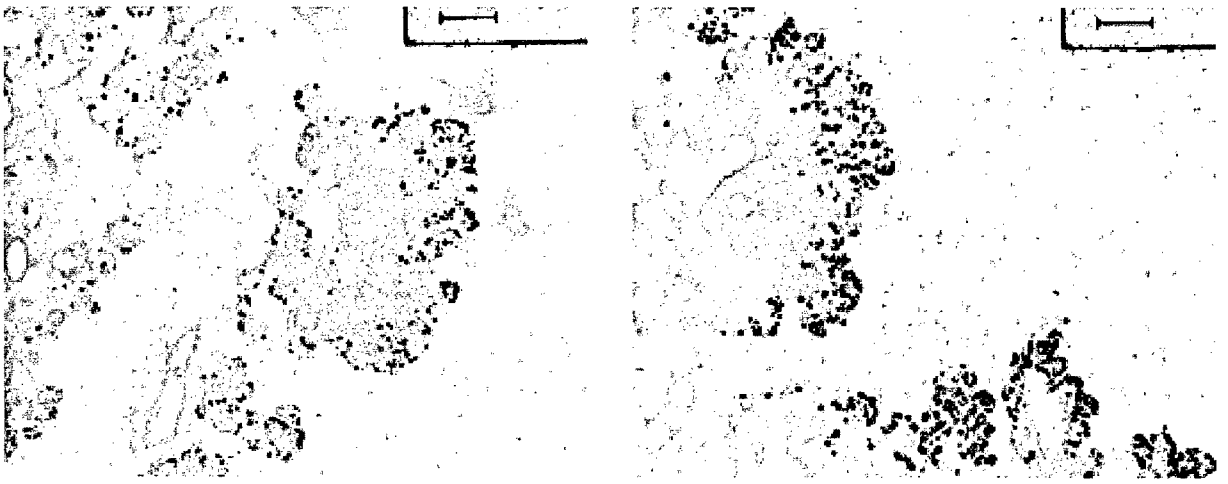

+/Csfm^{op} *Csfm^{op}/Csfm^{op}*

B.

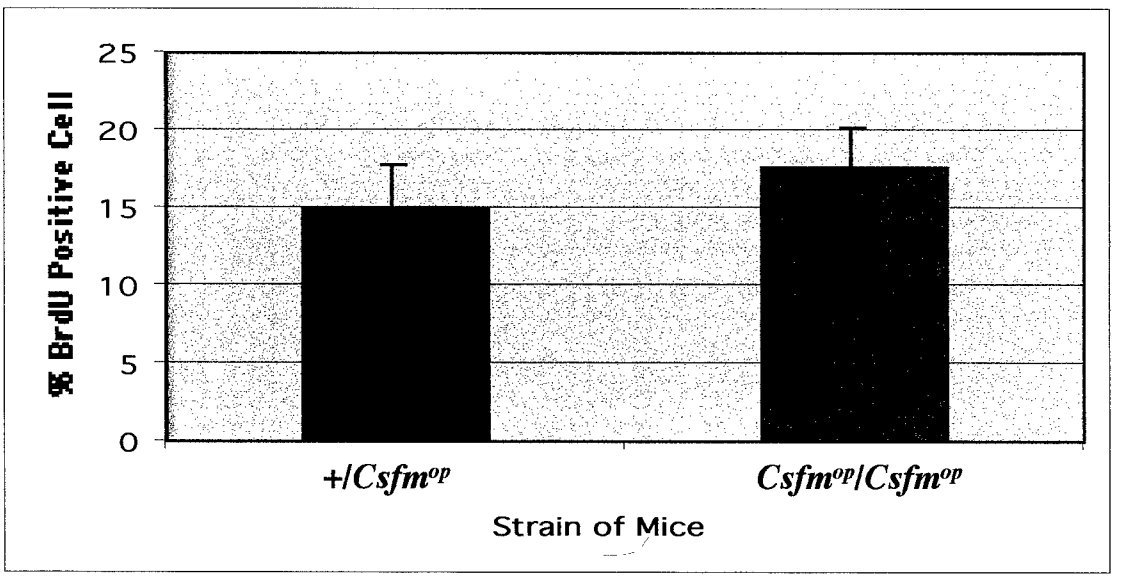

P: 0.48311
n = 6

Figure 5

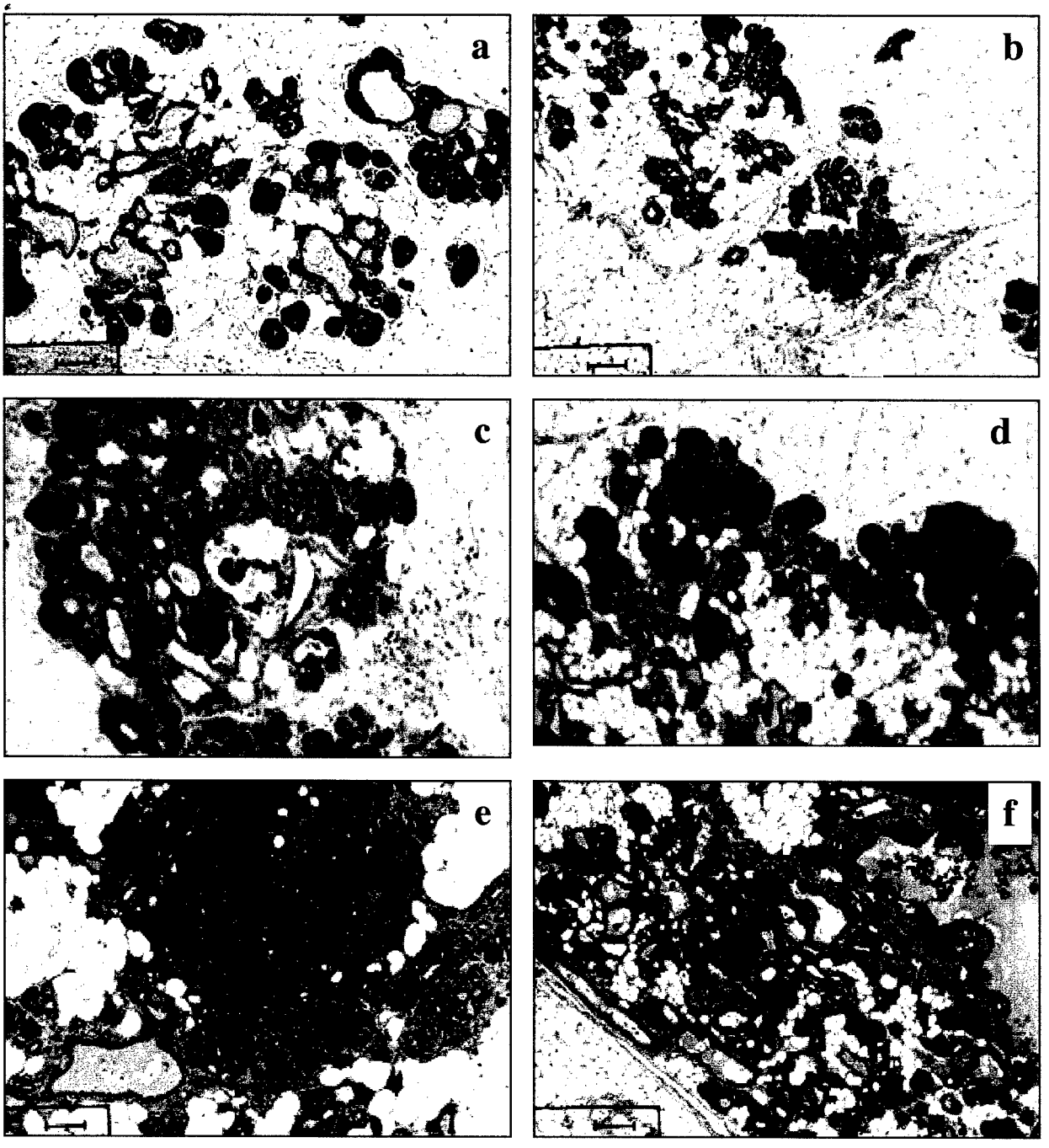

Figure 6

Primary Tumor Histology

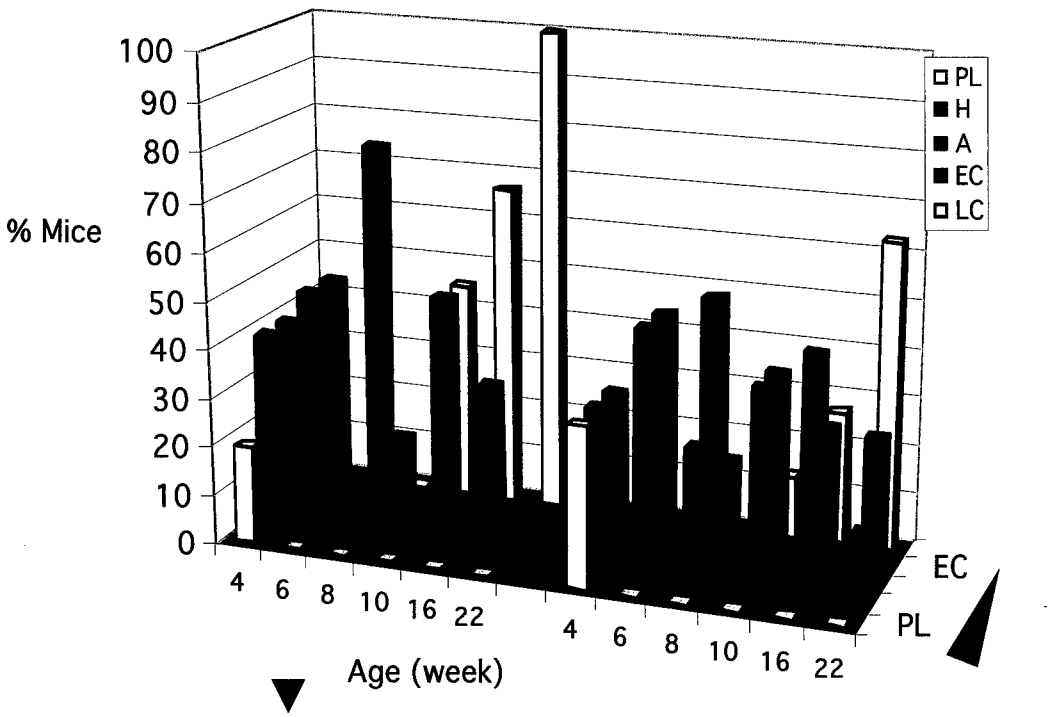

	4	6	8	10	16	22		4	6	8	10	16	22
□PL	20	0	0	0	0	0		33	0	0	0	0	0
■H	40	50	7.1	9.1	0	0		33	50	27	13	0	0
■A	40	50	79	0	5.6	0		33	50	55	38	46	11
■EC	0	0	14	46	28	0		0	0	18	38	27	26
□LC	0	0	0	46	67	100		0	0	0	13	27	63

+/Csfm^{op} ***Csfm^{op}/Csfm^{op}***

Figure 7

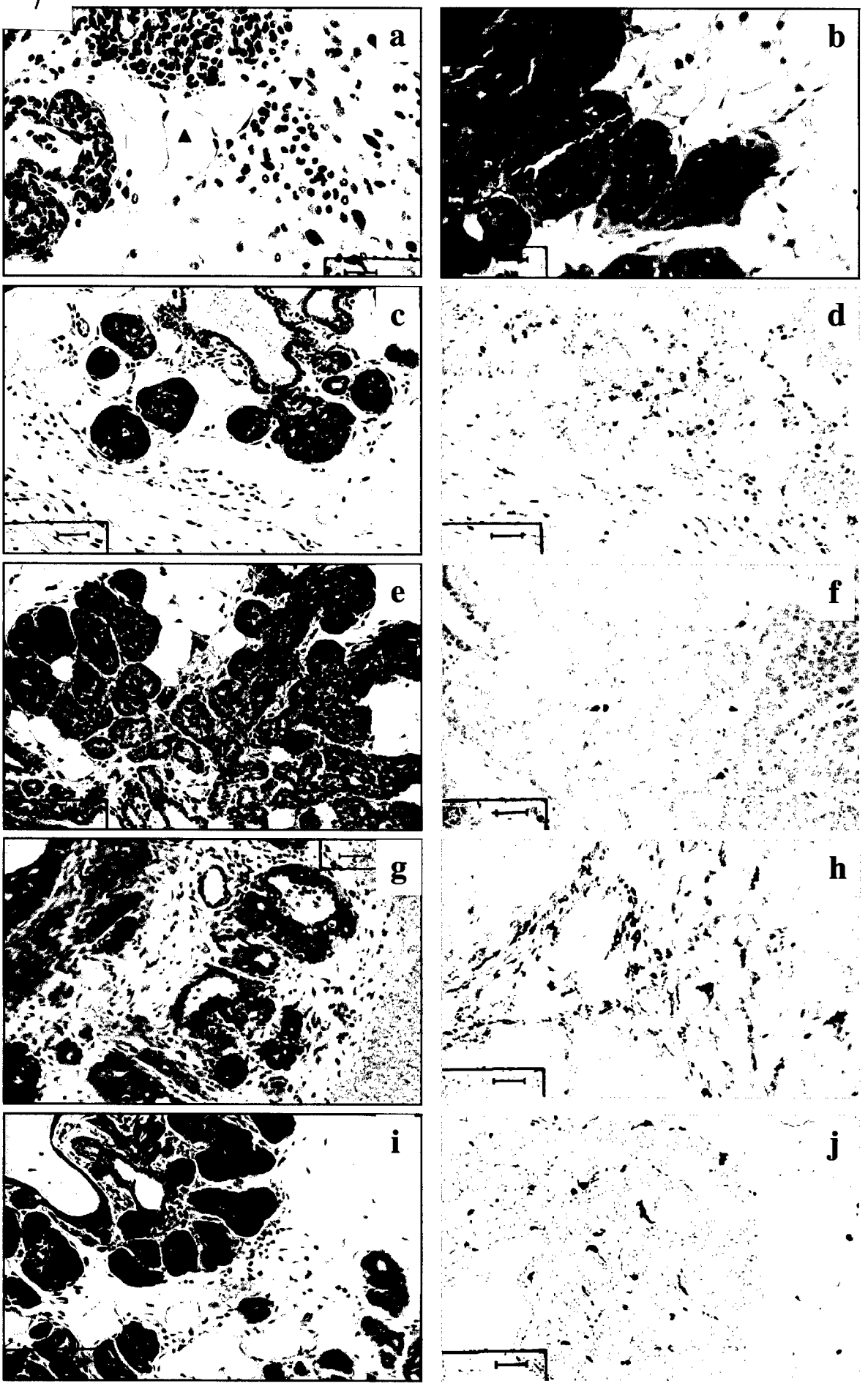

Figure 8

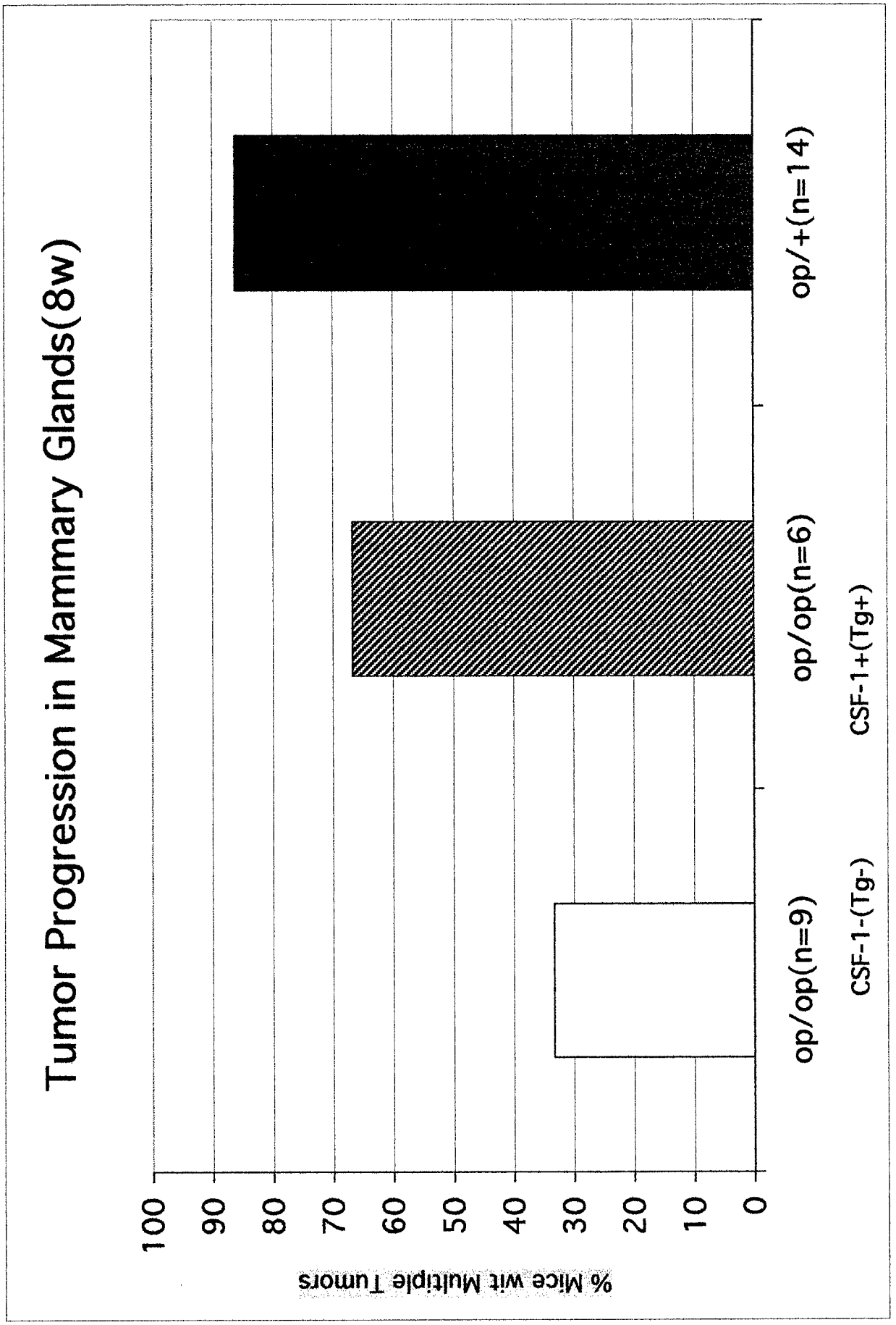
Tumor Progression in Mammary Glands(8w)
% Mice wit Multiple Tumors
100
90
80
70
60
50
40
30
20
10
0
op/op(n=9)
op/op(n=6)
op/+(n=14)
CSF-1-(Tg-)
CSF-1+(Tg+)

Figure 9

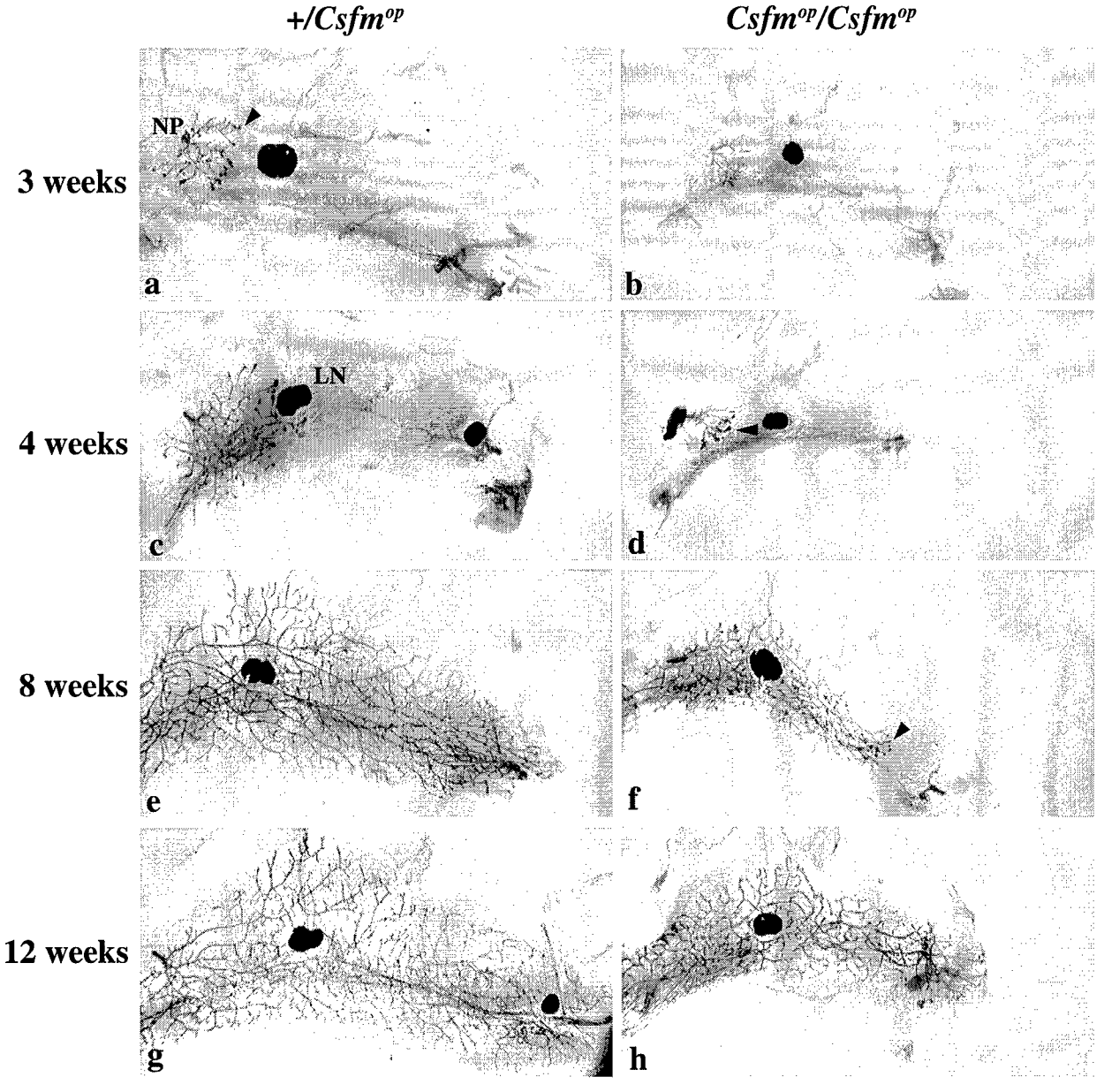
+/Csfm^op
Csfm^op/Csfm^op
3 weeks
4 weeks
8 weeks
12 weeks
NP
LN
a
b
c
d
e
f
g
h

Figure 10

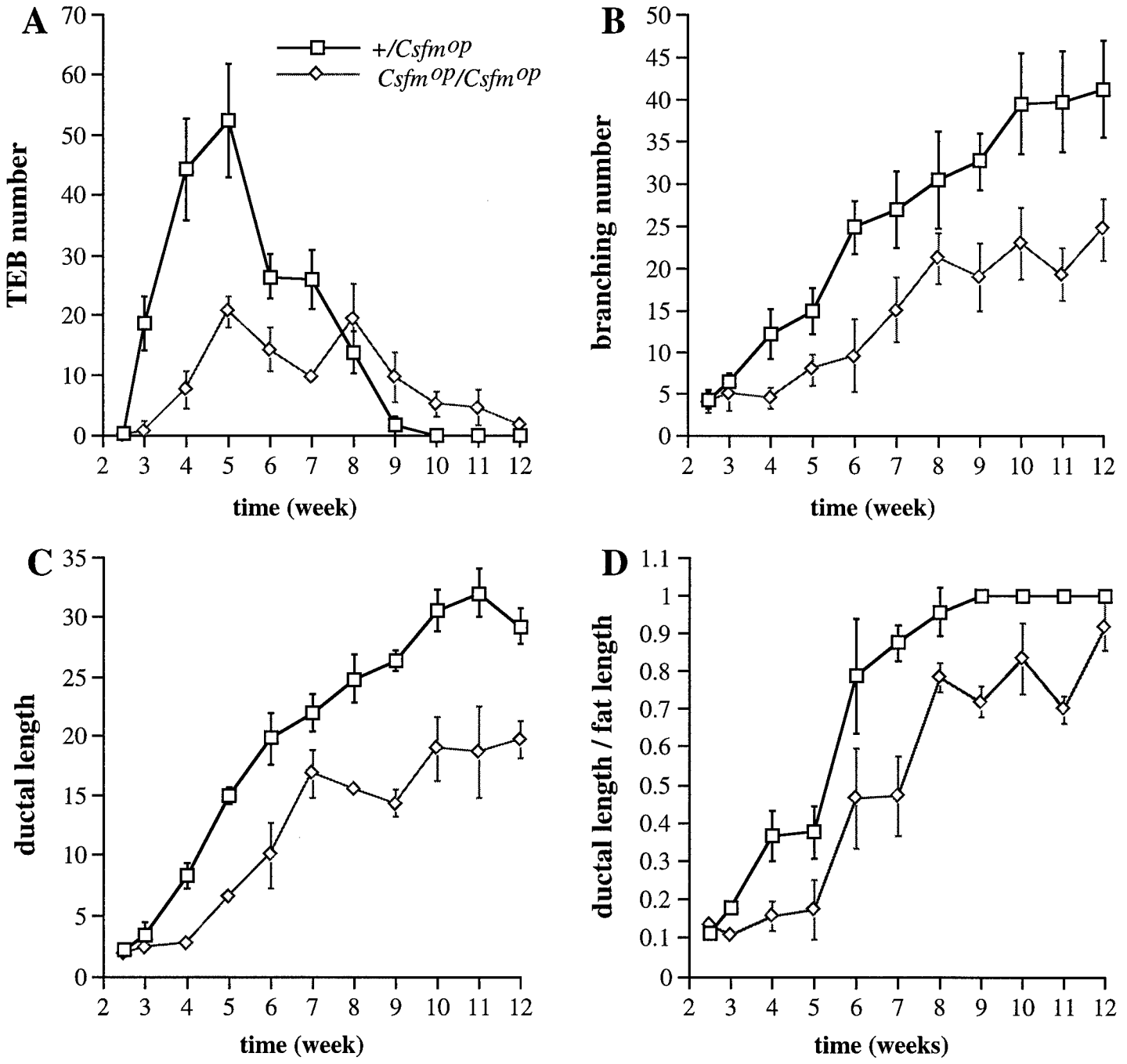
A
TEB number
+/Csfm^op
Csfm^op/Csfm^op
time (week)
B
branching number
time (week)
C
ductal length
time (week)
D
ductal length / fat length
time (weeks)

Figure 11

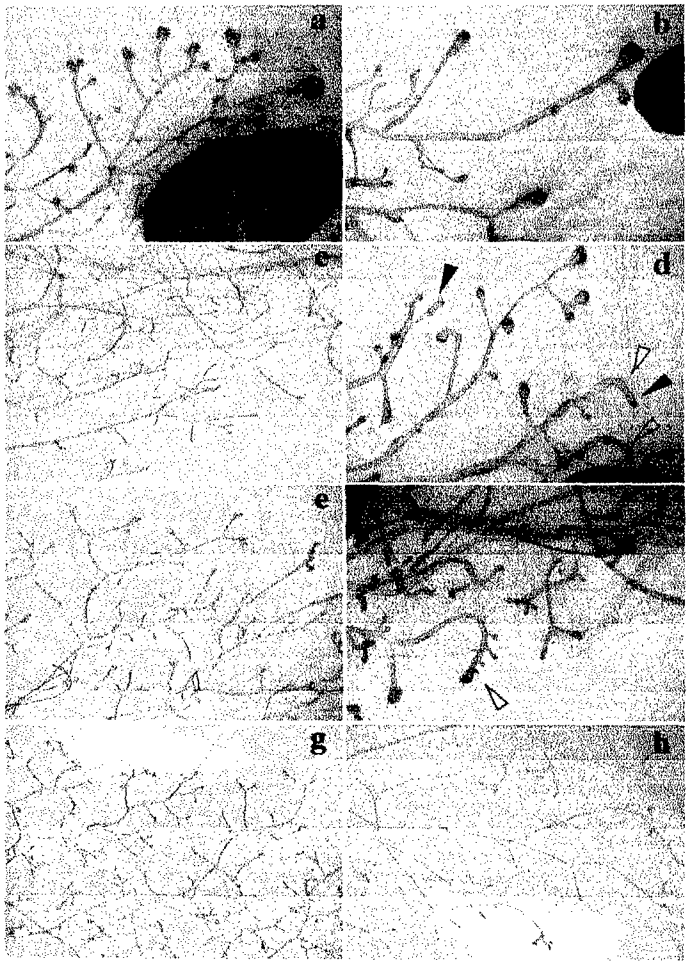

Figure 12

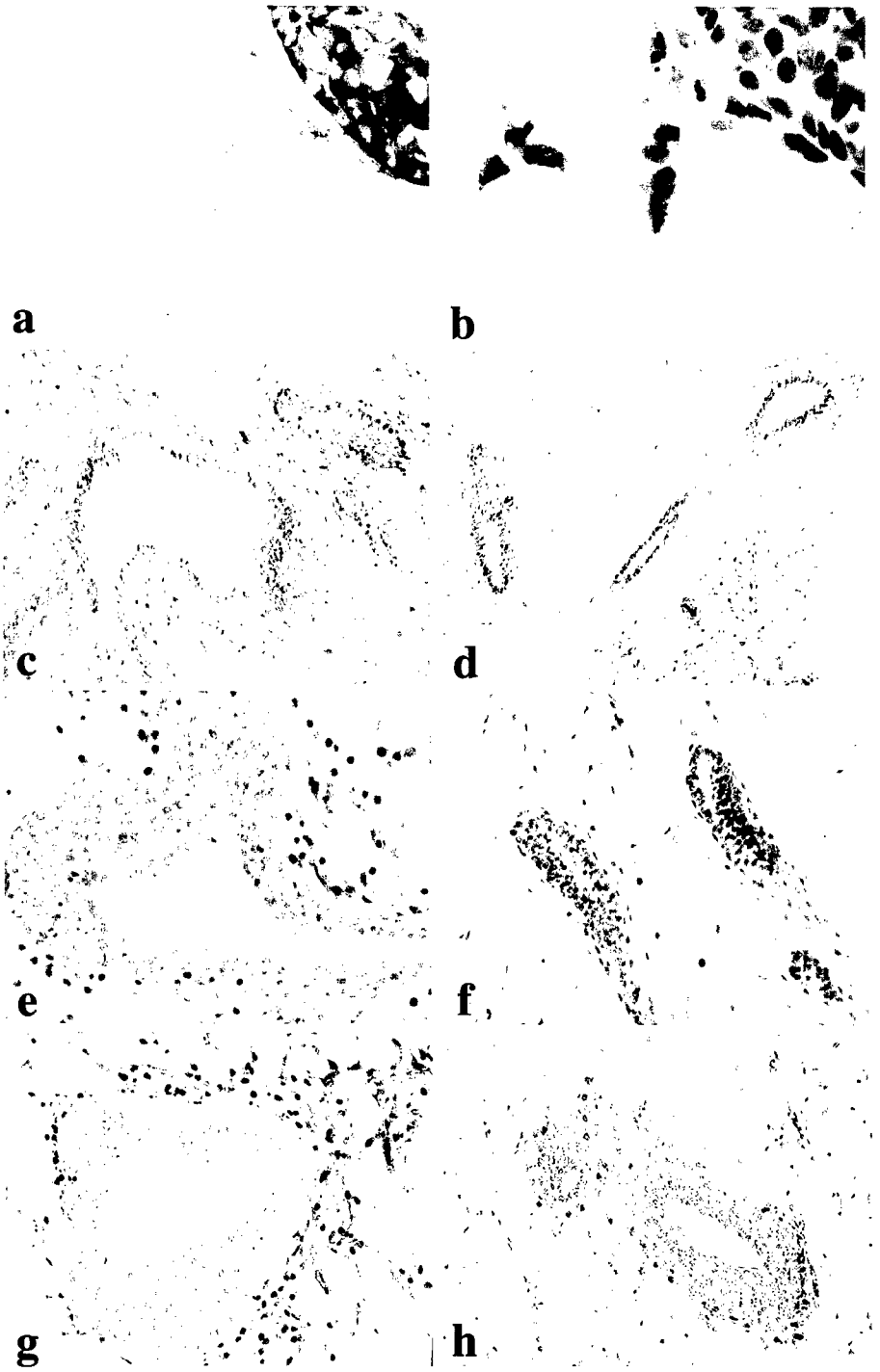

Figure 13

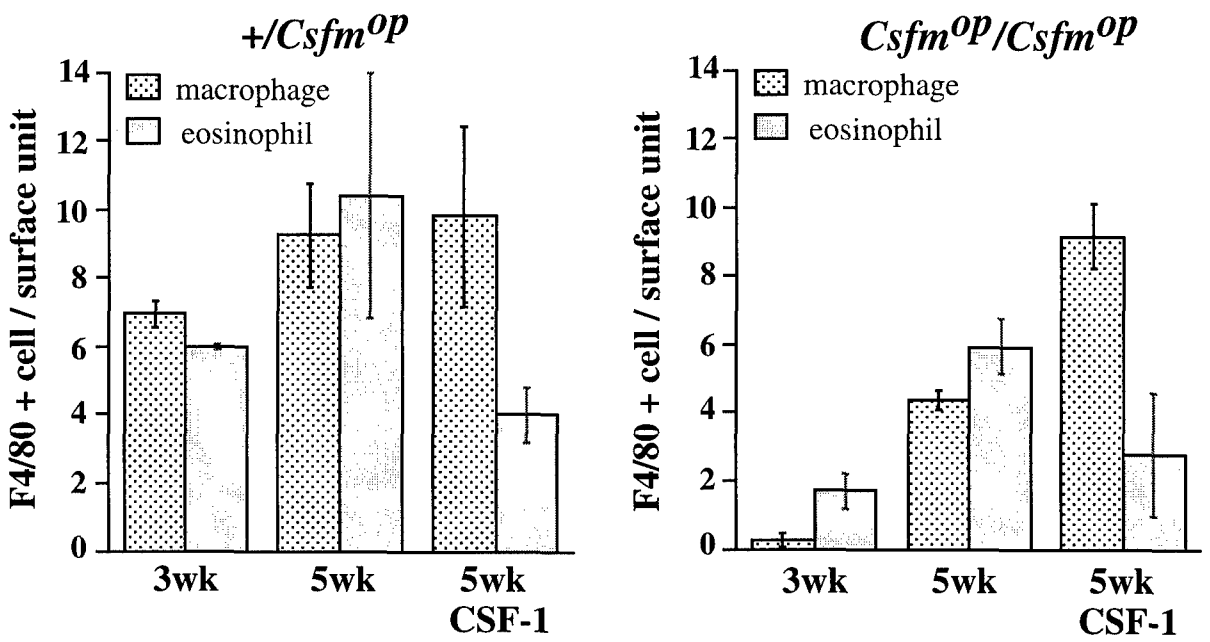
+/Csfm^op
Csfm^op/Csfm^op
macrophage
eosinophil
F4/80 + cell / surface unit
0
2
4
6
8
10
12
14
3wk
5wk
5wk CSF-1

Figure 14

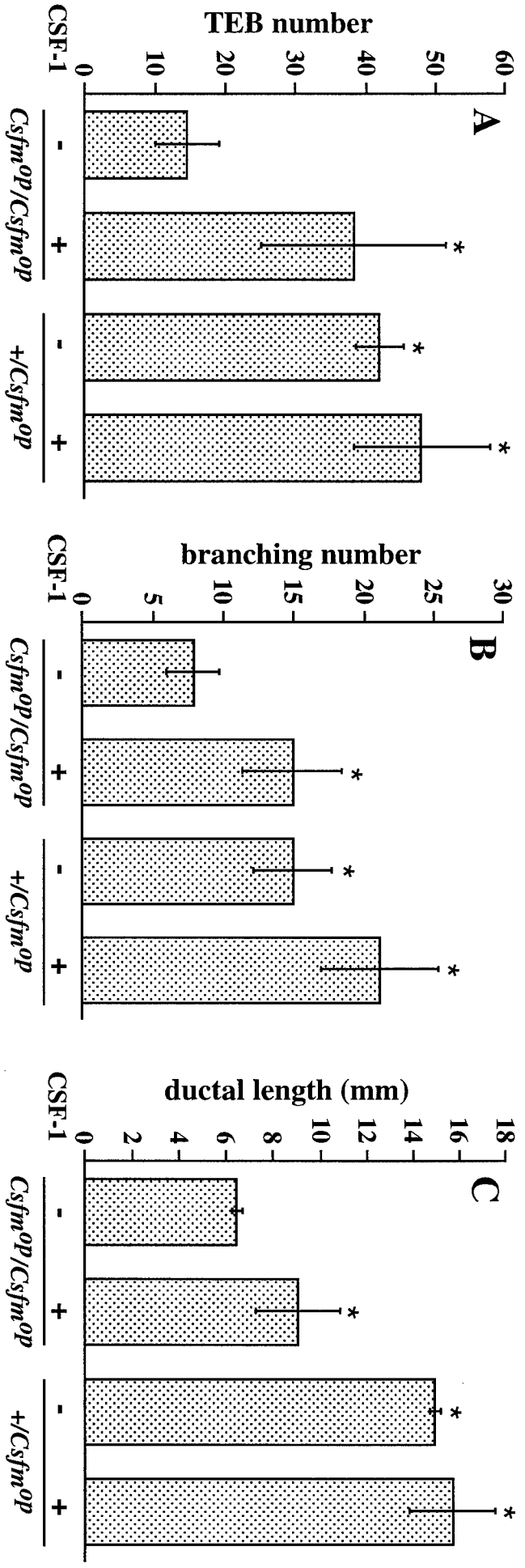
TEB number
A
CSF-1
Csfm^op/Csfm^op
+/Csfm^op
branching number
B
ductal length (mm)
C

Figure Legend

Figure 1. Whole mount analysis of mammary tumor progression in MMTV-PYVmT transgenic mice. Representative slides from a whole mount preparation of right abdominal mammary glands of *+/Csfm^{op}* (a, c, e and g) or *Csfm^{op}/Csfm^{op}* transgenic mice (b, d, f and h) at 4(a and b), 10(c and d), 12(e), and 16(f), 18(g) and 17 weeks (h). The primary tumors, the focus found in young mice as a single focus, is indicated by the arrow.

Figure 2. Tumor progression in MMTV/PYVmT transgenic mice. A. Comparison of multiple tumor formation in *+/Csfm^{op}* and *Csfm^{op}/Csfm^{op}* MMTV/PYVmT transgenic mice. Data are presented as the percentage of mice developed multiple mammary tumors at the age indicated and the result was obtained from the whole mount analysis of the right abdominal mammary glands. Mice carrying more than one focus in the mammary gland were classified as having multiple mammary tumors. Transgenic mice in *+/Csfm^{op}* or *Csfm^{op}/Csfm^{op}* background were labeled as op/+ or op/op respectively. **B.** Comparison of the formation of confluent mammary tumors. The percentages of *+/Csfm^{op}* and *Csfm^{op}/Csfm^{op}* transgenic mice developed confluent mammary tumors (>70 foci/gland) were examined at the same tumor progression stage, defined with respect to the initiation of the plateau in Fig. 2A. 0 to 6 weeks on the plateau in Fig. 2A represented 8 to 14 weeks for *+/Csfm^{op}* (op/+) and 14 to 20 weeks for *Csfm^{op}/Csfm^{op}* (op/op) mice. **C.** Comparison of primary tumor growth. The sizes of the primary tumors were measured using NIH Image 1.61 on the whole mount mammary gland preparation at the age indicated. Data are presented as the mean $\pm$ SE of at least three individual mice in each group. Samples from *+/Csfm^{op}* and *Csfm^{op}/Csfm^{op}* PYVmT transgenic mice are labeled as op/+ and op/op respectively. **D.** Distant metastasis of mammary tumors. Northern analysis of PYVmT RNA expression in metastatic mammary tumors in lungs of MMTV/PYVmT transgenic mice at the ages indicated. Data are presented as mean $\pm$ SE of at least three individual mice/point. Samples from *+/Csfm^{op}* and *Csfm^{op}/Csfm^{op}* mice are labeled as op/+ and op/op respectively.

Figure 3. A. Comparison of mammary gland development between *+/Csfm^{op}* and *Csfm^{op}/Csfm^{op}* PYVmT transgenic mice. The development of the mammary gland was measured as the ratio of the length of the epithelial tree to that of the fat pad. All of the measurements were based on the whole mount preparation of abdominal mammary glands. Data are presented as the mean + SE of individual mice/group as indicated. Samples from *+/Csfm^{op}* and *Csfm^{op}/Csfm^{op}* mice are labeled as op/+ and op/op respectively. **B.** Expression of PYVmT RNA in mammary gland epithelium. Northern analysis of PYVmT RNA expression in mammary glands of *+/Csfm^{op}* or *Csfm^{op}/Csfm^{op}* MMTV-PYVmT transgenic mice (labeled as op/+ and op/op respectively) from age 6 to 12 weeks. The RNA blots were hybridized with both PYVmT and Keratin 18 cDNA probes and the hybridization signals of PYVmT from each individual mouse was normalized with keratin 18. No significant difference was found between means of *+/Csfm^{op}* and *Csfm^{op}/Csfm^{op}* (*t test*, $p = 0.211275$). Data are presented as the mean $\pm$ SE of eight individual mice in each group.

Figure 4. Comparison of tumor cell proliferation. A. BrdU incorporation in mammary tumors at 8 weeks. Female MMTV-PYVmT transgenic mice were given BrdU intraperitoneally 2 hr before sacrifice and formalin fixed abdominal mammary glands was immunostained for BrdU. Shown are primary tumors from heterozygous or homozygous CSF-1 null mutant mice (*+/Csfm^{op}* or *Csfm^{op}/Csfm^{op}*) (magnification x 100). **B.** Comparison of BrdU incorporation between *+/Csfm^{op} and Csfm^{op}/Csfm^{op}* primary tumors. The entire primary tumors in BrdU stained mammary glands were scanned and the BrdU+ cells, as a fraction of the total scanned area, were determined using NIH Image 1.61. No significant difference was found in BrdU+ cell/total cell between *+/Csfm^{op}* and *Csfm^{op}/Csfm^{op}* (*t test, p = 0.48311*). Data are presented as the mean $\pm$ SE of six individual mice in each group.

Figure 5. Histological progression of primary tumors in MMTV-PYVmT transgenic mice. Formalin fixed abdominal mammary glands from either *+/Csfm^{op}* (a, c and e) or *Csfm^{op}/Csfm^{op}* MMTV-PYVmT transgenic mice (b, d and f) were stained with hematoxylin and eosin. a, and b; c and d; e and f; were from mice at 7, 9 and 10 weeks respectively. Shown are the primary mammary tumors (magnification x100).

Figure 6. A. Histopathological progression of primary tumors. The histopathological stage of the primary tumors was defined as described in the Material and Methods. PL, H, A, EC and LC represent following histopathologic stages: proliferative lesion, hyperplacia, adenoma, early carcinoma, and late carcinoma. The histopathologic progression of the primary tumors in *+/Csfm^{op}* and *Csfm^{op}/Csfm^{op}* mice presented as the distribution of mice at various stages at the age indicated. The red arrow indicated the degree of the tumor progression from early (PL) to late stages (EC). A significant advance of *+/Csfm^{op}* primary tumors at 10 weeks as indicated by the green arrow.

Fig. 7. Infiltration of leukocytes and F4/80+ cells around mammary tumors. a to b, leukocytic infiltration in *+/Csfm^{op}* and *Csfm^{op}/Csfm^{op}* mammary glands at 9 weeks. Shown is a focal leukocytic infiltration site next to the primary mammary tumor in a *+/Csfm^{op}* PYVmT transgenic mouse (a) and the primary tumor in a *Csfm^{op}/Csfm^{op}* littermates(b)(magnification x400). The areas with lost of basement membrane on the *+/Csfm^{op}* tumor are indicated by arrows. c to f, the infiltration of leukocytes and F4/80+ cells around the primary tumors in mammary glands of *+/Csfm^{op}* and *Csfm^{op}/Csfm^{op}* PYVmT transgenic mice at 7 weeks . Shown are the histology (c and e) and immunohistology for F4/80+ cells (d and f) of primary mammary tumors in *+/Csfm^{op}* (c and d) and *Csfm^{op}/Csfm^{op}* mammary glands (e and f)(magnification x250). g to j, mammary tumors at late carcinoma stage(magnification x250). Shown are representative slides of mammary tumors at late carcinoma stage in a in *+/Csfm^{op}* PYVmT transgenic mouse at 19 weeks (histology, g; and immunohistochemistry for F4/80, h) and a *Csfm^{op}/Csfm^{op}* mouse at 20 weeks(histology, i; and immunohistochemistry for F4/80, j). For histologic analysis, mammary glands were fixed in formalin and stained with

hematoxylin and eosin. Immunohistochemical staining for F4/80 cells was described in the Materials and Methods.

Fig. 8. The effect of CSF-1 expression on mammary tumor progression in *Csfm^{op}/Csfm^{op}* mice. Data are presented as the percentage of mice developed multiple mammary tumors at 8 weeks. *Csfm^{op}/Csfm^{op}* PYVmT transgenic mice expressing CSF-1 transgene was labeled as op/op CSF-1(Tg+) and the control *Csfm^{op}/Csfm^{op}* PYVmT transgenic mice, which carried the incomplete CSF-1 transgene, was labelled op/op CSF-1(Tg-). Data were obtained from a whole mount analysis of abdominal mammary glands prepared from 8-week old MMTV-PYVmT transgenic mice carrying heterozygous or homozygous CSF-1 null-mutation (+/*Csfm^{op}* or *Csfm^{op}/Csfm^{op}*, op/+ or op/op respectively).

Figure 9: Whole-mounts of mammary glands from +/*Csfm^{op}* and *Csfm^{op}/Csfm^{op}* mice. Whole mount preparations are shown of +/*Csfm^{op}* and *Csfm^{op}/Csfm^{op}* virgin mice of 3, 4, 8 and 12 weeks of age. The photomicrographs were taken at the same magnification of the entire fourth abdominal mammary gland, showing the atrophic development in *Csfm^{op}/Csfm^{op}* mice. The arrow indicates TEB, NP is the nipple area and LN the lymph node of the mammary gland.

Figure 10: Ductal length, branching, terminal end bud (TEB) numbers and the relative ductal growth in the mammary glands of +/*Csfm^{op}* and *Csfm^{op}/Csfm^{op}* mice. Mice were sacrificed at 2.5 to 12 weeks of age, and the fourth abdominal mammary gland whole mounts were analyzed. The ductal length (mm) is measured from the nipple area to the tip of the 3 longest ducts through the lymph node, the fat length is similarly measured from the nipple area to the tip of the fat pad. Branching number is the mean of branching numbers along the 3 longest ducts from the nipple area to the migration front of TEBs. TEBs are enumerated in the whole mammary glands. Points represent mean +/- SD of at least three mice per time point.

Figure 11: Branching morphogenesis of mammary gland whole mount preparations of +/*Csfm^{op}* and *Csfm^{op}/Csfm^{op}* mice. Light micrographs of mammary gland whole mounts from +/*Csfm^{op}* (a, c, e, g) and *Csfm^{op}/Csfm^{op}* (b, d, f, h) mice at 5 (a, b), 6 (c, d), 8 (e, f), and 12 (g, h) weeks of age. All the pictures are positioned in the same direction from left to right, the nipple area to the tip of the fat pad respectively. Figures a and b represent the ductal migration front at 5 weeks of age, Figures c to h, the branching tree near the limit of the fat pad. Black arrows indicate TEDs without large-club end formations and blank arrows show the disorganized TEDs orientated in the opposite direction to the TEB migration front.

Figure 12: F4/80 immunohistochemistry of mammary glands sections of +/*Csfm^{op}* and *Csfm^{op}/Csfm^{op}* mice. The same TEB section was first stained with giemsa (a) and secondly immunostained with the antibody anti-F4/80 (b), showing polynuclear eosinophils characterized by their pink cytoplasmic granules as F4/80 positive cells. Immunostaining of F4/80 positive macrophages and eosinophils in mammary glands from

14 days (c, d), 3 weeks (e, f) and 5 weeks (g, h) of age mice. Mammary gland sections of control mice (c, e, g) and CSF-1 null mutant mice (d, f, h) were immunostained with the anti-F4/80 antibody and positive cells were detected with a peroxidase-coupled detection system (brown coloration). Sections were counterstained with hematoxylin. Nipple areas (c, d), terminal end buds (e, g, h) and terminal end ducts (f) are shown. Original magnification, a, b, 1000X; c, d, g, h, 250X; e, f, 400X.

Figure 13: Enumeration of macrophages and eosinophils around TEBs.
Enumeration of macrophages and eosinophils around TEBs in +/*Csfm*^{op} and *Csfm*^{op}/*Csfm*^{op} mice treated and untreated with CSF-1 from birth. F4/80 immunohistochemistry were performed on mammary gland sections followed by a weak hematoxylin/eosin counterstaining in order to distinguish eosinophils from macrophages. F4/80 positive cells were counted per surface units (1000X magnification) around at least 3 TEBs of 3 to 5 mice per group. Mammary glands of untreated mice were analyzed at 3 and 5 weeks of age, while mammary glands of 5 daily CSF-1-treated mice per group were similarly examined. Note the reduced number of macrophages in mutant mice which is restored after CSF-1 treatment from birth.

Figure 14: Ductal length, branching and terminal end bud (TEB) in the mammary glands of CSF-1 treated +/*Csfm*^{op} and *Csfm*^{op}/*Csfm*^{op} mice. Ductal length, branching and TEB numbers are enumerated in the whole mount mammary glands of +/*Csfm*^{op} and *Csfm*^{op}/*Csfm*^{op} mice without (-) or with (+) daily CSF-1 treatment from birth. Mice treated with daily CSF-1 injection from birth and their untreated littermates were sacrificed at 5 weeks of age. The fourth abdominal mammary gland whole mounts were analyzed as previously in figure 11. Note the rescue of TEB and branching number in CSF-1 treated *Csfm*^{op}/*Csfm*^{op} mice. Points represent mean +/- SD of 5 mice per time point. * denotes significant variation from values obtained for untreated *Csfm*^{op}/*Csfm*^{op} mice ($p<0.01$).

Table 1. Development of Multiple Mammary Tumors

+/Csfm^{op}

	8w	10w	12w	14w
Confluent/ Total (%)	4/22 (18%)	8/11 (73%)	11/11 (100%)	7/8 (97%)
Average Foci/gland (mice #)	20 (18)	29 (3)	-	19(1)

Csfm^{op}/Csfm^{op}

	14w	16w	18w	20w
Confluent/ Total (%)	1/7 (14%)	3/8 (43%)	2/5 (40%)	2/5 (60%)
Average Foci/gland (mice #)	4(6)	3 (5)	26(3)	14(3)

SALARIED PERSONNEL

Valerie Gouon, Ph.D.
Research Associate

Jim Lee
Research Technician

Xiamong Chen
Research Technician

DEPARTMENT OF THE ARMY
US ARMY MEDICAL RESEARCH AND MATERIEL COMMAND
504 SCOTT STREET
FORT DETRICK, MARYLAND 21702-5012

REPLY TO
ATTENTION OF:

MCMR-RMI-S (70-1y)

21 JUN 2001

MEMORANDUM FOR Administrator, Defense Technical Information Center (DTIC-OCA), 8725 John J. Kingman Road, Fort Belvoir, VA 22060-6218

SUBJECT: Request Change in Distribution Statement

1. The U.S. Army Medical Research and Materiel Command has reexamined the need for the limitation assigned to technical reports. Request the limited distribution statement for reports on the enclosed list be changed to "Approved for public release; distribution unlimited." These reports should be released to the National Technical Information Service.

2. Point of contact for this request is Ms. Judy Pawlus at DSN 343-7322 or by e-mail at judy.pawlus@det.amedd.army.mil.

FOR THE COMMANDER:

Encl

PHYLLIS M. RINEHART
Deputy Chief of Staff for
Information Management

DAMD17-94-J-4413	ADB261602
DAMD17-96-1-6112	ADB233138
DAMD17-96-1-6112	ADB241664
DAMD17-96-1-6112	ADB259038
DAMD17-97-1-7084	ADB238008
DAMD17-97-1-7084	ADB251635
DAMD17-97-1-7084	ADB258430
DAMD17-98-1-8069	ADB259879
DAMD17-98-1-8069	ADB259953
DAMD17-97-C-7066	ADB242427
DAMD17-97-C-7066	ADB260252
DAMD17-97-1-7165	ADB249668
DAMD17-97-1-7165	ADB258879
DAMD17-97-1-7153	ADB248345
DAMD17-97-1-7153	ADB258834
DAMD17-96-1-6102	ADB240188
DAMD17-96-1-6102	ADB257406
DAMD17-97-1-7080	ADB240660
DAMD17-97-1-7080	ADB252910
DAMD17-96-1-6295	ADB249407
DAMD17-96-1-6295	ADB259330
DAMD17-96-1-6284	ADB240578
DAMD17-96-1-6284	ADB259036
DAMD17-97-1-7140	ADB251634
DAMD17-97-1-7140	ADB259959
DAMD17-96-1-6066	ADB235510
DAMD17-96-1-6029	ADB259877
DAMD17-96-1-6020	ADB244256
DAMD17-96-1-6023	ADB231769
DAMD17-94-J-4475	ADB258846
DAMD17-99-1-9048	ADB258562
DAMD17-99-1-9035	ADB261532
DAMD17-98-C-8029	ADB261408
DAMD17-97-1-7299	ADB258750
DAMD17-97-1-7060	ADB257715
DAMD17-97-1-7009	ADB252283
DAMD17-96-1-6152	ADB228766
DAMD17-96-1-6146	ADB253635
DAMD17-96-1-6098	ADB239338
DAMD17-94-J-4370	ADB235501
DAMD17-94-J-4360	ADB220023
DAMD17-94-J-4317	ADB222726
DAMD17-94-J-4055	ADB220035
DAMD17-94-J-4112	ADB222127
DAMD17-94-J-4391	ADB219964
DAMD17-94-J-4391	ADB233754